

## CHAPTER V

### SORPTION AND TRANSPORT OF $Pb^{2+}$ , $Ni^{2+}$ , $Mn^{2+}$ , AND $Zn^{2+}$ UNDER BINARY AND MULTI-METAL SYSTEMS THROUGH LATERITIC SOIL: COLUMN EXPERIMENTS AND MODELING

#### Abstract

This study investigates the sorption and transport of four metals (i.e.,  $Pb^{2+}$ ,  $Ni^{2+}$ ,  $Zn^{2+}$ , and  $Mn^{2+}$ ) through lateritic soils at pH 5 in binary metals and multi-metal systems. Based on the breakthrough times of  $Pb^{2+}$  in single metal systems,  $Pb^{2+}$  was retained in lateritic soil more than to other metals ( $Ni^{2+}$ ,  $Zn^{2+}$ , and  $Mn^{2+}$ ). The retardation factors and average maximum sorption capacity of  $Pb^{2+}$  were found to be higher than other metals for the single, binary, and multi-metal systems. This may be due to the smaller hydrated radius of  $Pb^{2+}$  as compared to the other three metals. The presence of other metals ( $Ni^{2+}$ ,  $Zn^{2+}$ , and  $Mn^{2+}$ ) in the system, resulted in the reduction of sorption capacities of individual metals in both binary and multi-metal system. The HYDRUS-1D with local equilibrium convection-dispersion model (linear and Langmuir isotherm) and nonequilibrium (two-site model, TSM) was applied to describe heavy metal breakthrough curves under binary and multi-metal systems. The results showed that a two-site model (TSM) with first order kinetic were able to describe the breakthrough curves better than the local equilibrium convection-dispersion model both in binary and multi-metal systems. The fraction of instantaneous site ( $f$ ) of each metal on the lateritic soil in the binary and multi-metal systems was consistently about 30-58 % of sorption site. The model results also suggested that  $Pb^{2+}$  was more strongly sorbed than other metals under single, binary, and multi-metal systems. In the presence of other metals, the maximum sorption capacity of  $Pb^{2+}$  decreased indicating possible competition for sorption sites with other metals.

**Keywords:** heavy metals; sorption; HYDRUS-1D; two-site model; lateritic soil

## 5.1 Introduction

The transport of heavy metals through soil has been investigated with great interest by both environmental and soil scientists. Heavy metals in wastes generated by anthropogenic and natural activities can leach and contaminate soils and groundwater systems (Protano and Riccobono, 1997; Macro et al., 2002; Passariello, 2002; Ramirez Requielme et al., 2002; Lottermoser, 2003; Abut et al., 2003). Pollution from heavy metals is a very serious threat not only to environment but also to human health due to their toxicity, persistency and non-degradability. These metals include but not limited to Cr, Mn, Ni, Zn, Cu, Pb, As, Cd, and Hg. For example, within a zone of 1 km from a copper mining and smelting site in southwestern Poland, Roszyk and Szerszen (1998) found that the soil contained 250 to 10,000 mg kg<sup>-1</sup> of Cu, 90 to 18,000 mg kg<sup>-1</sup> of Pb, 0.3 to 10.9 mg kg<sup>-1</sup> of Cd, and 55 to 4,000 mg kg<sup>-1</sup> of Zn. Mining activities generally release substantial amounts of wastes, caused by poorly designed and maintained storage facilities, poor environmental management of mining wastes and the consequences of acid mine drainage (Lottermoser, 2003).

An understanding of the sorption and transport behavior of heavy metals is essential to assess the extent of contamination through subsurface aquifer for a contaminated site. Mining soils, when removed from the subsurface, are rapidly oxidized and become acidic, leaching large quantities of cations such as calcium, manganese, and iron. Batch sorption experiments are typically performed to investigate the impact of two or more metals on the sorption to the soils. Batch sorption studies of Pb and Cd onto four soils from Spain conducted by Serrano et al. (2005) showed that soil with higher pH and clay content had the greatest sorption capacity as estimated by the maximum sorption parameters of the Langmuir model. Sorption of Pb was greater than that of Cd for all soils and the simultaneous presence of both metals tend to decrease their sorption although Cd sorption decreased more than that of Pb. Arias et al. (2006) conducted sorption of Cu and Zn onto acid soils at pH 5 and found that sorption can be described by the Freundlich equation rather than by the Langmuir equation. They found that the total metal sorption from solutions containing Cu and Zn in 1:1 mole ratio was intermediate between sorption from individual Zn and Cu solutions of the same total concentration.

Column experiments can be used as an alternative to investigate the sorption and transport of metals. Column experiments can be used to investigate the displacement of dissolved solutes through soil and are considered to reflect field conditions more closely than batch studies and may provide information that are not available using equilibrium batch experiments (Williams et al., 2003; Pang et al., 2004; Miretzky et al., 2006; Yolcubal and Akyol, 2007). Although for many contaminated sites, there are more than one metal in the contaminated plume, most column studies on heavy metal sorption are mostly focused on one metal system (Kookana and Naidu, 1998; Li, 2000; 2001; Williams et al., 2003; Pang et al., 2004; Miretzky et al., 2006; Yolcubal and Akyol, 2007). The few papers on sorption of heavy metals in multi-metal systems include the work done by Pazko, T. (2003) where they studied competitive sorption of  $\text{Cu}^{2+}$ ,  $\text{Co}^{2+}$ , and  $\text{Cr}^{3+}$  onto grey-brown podzolic soils using batch and column techniques. They showed that the Freundlich equation described the batch sorption experiments well and the linear sorption equation was successfully applied to describe  $\text{Cr}^{3+}$  and  $\text{Cu}^{2+}$  sorption in column experiments.  $\text{Cu}^{2+}$  and  $\text{Cr}^{3+}$  on  $\text{Co}^{2+}$  sorption had a significant effect in both column and batch experiments. In the batch and column studies by Rodríguez-maroto (2003), it was shown that Pb was more preferentially sorbed than Cd onto agricultural soil and Langmuir isotherms including competitive sorption isotherms obtained from batch experiments were able to predict column experimental results well. However, some of the issues with multi-metal systems include the possible interactions between heavy metals for sorption sites, non-equilibrium sorption and mass transfer of metals, which are not completely known.

The objectives of this study are to investigate the influence of one or more heavy metals in mine tailings leachate and their concentrations on the retention and mobility of heavy metals through lateritic soil. To accomplish these objectives, column studies were conducted to investigate the transport of simultaneous heavy metals in binary and multi-metal systems in lateritic soils. The transport of these heavy metals under different conditions was described using HYDRUS-1D, a local convection-dispersion equilibrium model with linear and nonlinear (Langmuir) isotherm and nonequilibrium two-site model (TSM). Information obtained from this study will lead to a more accurate prediction of the migration of heavy metals from these sites and assist in selecting appropriate strategies in remediating/monitoring the contaminated site.

## 5.2 Materials and Methods

### 5.2.1 Soil samples and reagents

The lateritic soils used and its properties were presented in Section 4.2 of Chapter 4.

The four metal species used in the experiments were prepared by dissolving 0.1 M of  $\text{Pb}(\text{NO}_3)_2(\text{s})$ ,  $\text{Zn}(\text{NO}_3)_2 \cdot 6\text{H}_2\text{O}(\text{s})$ ,  $\text{Ni}(\text{NO}_3)_2 \cdot 6\text{H}_2\text{O}(\text{s})$ , and  $\text{MnCl}_2 \cdot 4\text{H}_2\text{O}(\text{s})$  in separately distilled water. The stock solutions were mixed to obtain solutions with more than one metal, with 0.01 M NaAc ( $\text{CH}_3\text{COONa}$ ;  $pK_a = 4.76$ ,  $MW = 136.08 \text{ g mol}^{-1}$ ) as a buffer solution. NaOH and  $\text{HNO}_3$  were used for final pH adjustment to maintain pH 5.

### 5.2.2 Tracer and heavy metals transport experiments

Soil samples were uniformly packed in acrylic columns with an inner diameter of 2.50 cm and a depth of 10 cm. The soil column was initially saturated with deionized water from the bottom with at least 6 pore volumes (PVs) to eliminate the entrapped air and to minimize the possibility of preferential flow (Pang et al., 2004). Due to the very fine texture of the lateritic soil, the wet soil could not be compacted to a typical field soil bulk density. A bulk density about  $1 \text{ g cm}^{-3}$  was obtained. After the saturation procedure, a solution of  $30 \text{ mg L}^{-1}$  of bromide ( $\text{Br}^-$ ) was injected from the bottom at a rate of  $8 \pm 0.5 \text{ mL hr}^{-1}$  and the column effluent was collected using a fraction collector. The effluent was filtered and analyzed using ion chromatography. After injecting the  $\text{Br}^-$ , about 6 PVs of NaAc buffer solution were injected to maintain a constant pH of 5. The mixed metal solution was then injected from bottom of column and the effluent collected periodically to monitor the concentrations of metals and pH in the effluent. The metal concentrations in the effluent were determined by flame atomic absorption spectrophotometry. The breakthrough curves (BTC), expressed as the relative concentrations ( $C/C_0$ ) versus pore volume ( $V/V_0$ ) were plotted, where  $C_0$  is the initial concentration added and  $V_0$  is the pore volume of soil column. The binary and multi-metal experiments conducted are presented in Table 5-



1.  $\text{Pb}^{2+}$  was used as the main metal while  $\text{Mn}^{2+}$ ,  $\text{Ni}^{2+}$  and  $\text{Zn}^{2+}$  were used as the second metal.

**Table 5.1** Column experiments for binary metal and multi-metal systems

System	Metals	Concentration ( $\text{mmol L}^{-1}$ )		
		$\text{Pb}^{2+}$	$\text{Mn}^{2+}$ or $\text{Ni}^{2+}$ or $\text{Zn}^{2+}$	pH
Binary metals	$\text{Pb}^{2+}$ - $\text{Mn}^{2+}$	5	3, 5, 10	5
	$\text{Pb}^{2+}$ - $\text{Ni}^{2+}$	5	3, 5, 10	5
	$\text{Pb}^{2+}$ - $\text{Zn}^{2+}$	5	3, 5, 10	5
Multi-metals	$\text{Pb}^{2+}$ -( $\text{Mn}^{2+}$ - $\text{Ni}^{2+}$ - $\text{Zn}^{2+}$ )	5	5/ 5/ 5	5

### 5.2.3 Transport Models

#### (a) CXTFIT

CXTFIT 2.0 (Torride et al., 1995) is a program with a number of analytical solutions for one-dimensional solute transport based on the convection-dispersion equation (CDE). CXTFIT includes an inverse modeling capability that uses a nonlinear least-squares parameter optimization method to fit mathematical solutions of the theoretical transport model to experimental data. The equilibrium CDE may be written as:

$$\frac{\partial C}{\partial t} = D_L \frac{\partial^2 C}{\partial x^2} - v_x \frac{\partial C}{\partial x} - \frac{\rho}{\theta} \frac{\partial C^*}{\partial t} \pm \left[ \frac{\partial C}{\partial t} \right]_{rxn} \quad (1)$$

where  $C$  = concentration of solute in liquid phase ( $\text{mg L}^{-1}$ );  $t$  = time (hr);  $D_L$  = longitudinal dispersion coefficient ( $\text{cm}^2 \text{hr}^{-1}$ );  $v_x$  = average linear groundwater velocity ( $\text{cm hr}^{-1}$ );  $\rho$  = bulk density of aquifer ( $\text{g cm}^{-3}$ );  $\theta$  = volumetric moisture content or porosity for saturated media;  $C^*$  = amount of solute sorbed per unit weight of solid ( $\text{mg g}^{-1}$ );  $rxn$  = subscript indicating a biological or chemical reaction of the solute (other than sorption) ( $\text{mg L}^{-1} \text{hr}^{-1}$ )

CXTFIT was applied to assess the transport parameters and to evaluate any physical nonequilibrium processes in the system using the linear equilibrium CDE model, (CD<sub>eq</sub>) and two-region nonequilibrium model (TRM). In the two-region model, the physical nature of the porous medium is separated into two domains: a mobile “dynamic” domain, and an immobile “stagnant” domain. Solute movement in the mobile regions occur by convection-dispersion model, whereas solute exchange between the two regions occurs by the first order diffusion. The governing equation for the two-region nonequilibrium model is:

$$(\theta_m + f\rho K_d) \frac{\partial c_m}{\partial t} + [\theta_{im} + (1-f)\rho K_d] \frac{\partial c_{im}}{\partial t} = \theta_m D_m \frac{\partial^2 c_m}{\partial x^2} - q \frac{\partial c_m}{\partial x} \quad (2)$$

$$[\theta_{im} + (1-f)\rho K_d] \frac{\partial c_{im}}{\partial t} = \alpha (c_m - c_{im}) \quad (3)$$

where the subscripts *m* and *im* refer to the mobile and immobile regions, respectively;  $\alpha$  is a first-order mass transfer coefficient (d<sup>-1</sup>), representing the rate of solute exchange between the mobile and immobile regions; and *f* is the fraction of mobile water. For nonsorbing solutes such as bromide (Br<sup>-</sup>), values of  $\beta$  and  $\omega$  can be used to evaluate potential contributions from physical nonequilibrium. Values for these nonequilibrium terms from the two-region model can be described as:

$$\beta = \frac{\theta_m + f\rho K_d}{\theta + \rho K_d} \quad (4)$$

$$\omega = \frac{\alpha L}{q} \quad (5)$$

Due to the limitation of CXTFIT program, it could apply only linear isotherm to describe the solute transport. However, sorption is generally not linear for heavy metals.

## (b) HYDRUS-1D

HYDRUS-1D can be applied to simulate transport of heavy metals in soils and the model code can be applied for different equilibrium and non-equilibrium flow and transport in both direct and inverse mode. The following were used in this study to assess experimental breakthrough curves (BTCs):

- Linear sorption model and nonlinear Langmuir sorption model for the equilibrium convection-dispersion transport model (Eq.2)
- Chemical non-equilibrium model or the two-site model (TSM) as presented by (Eq.7) (Selim et al., 1976). Using Langmuir sorption model, the governing equations for the two-site model becomes (Fetter, 1993) :

$$\left(1 + \frac{f\rho}{\theta} \left[ \frac{Q_{\max} b}{(1 + bC)^2} \right]\right) \frac{\partial c}{\partial t} = D \frac{\partial^2 c}{\partial x^2} - v \frac{\partial c}{\partial x} - \frac{\alpha\rho}{\theta} \left[ (1-f) \frac{Q_{\max} bC}{1 + bC} - s_2 \right] \quad (6)$$

where  $f$  is the fraction of equilibrium sites and  $\alpha$  is a first-order kinetic rate coefficient ( $d^{-1}$ ).  $S_2$  is solid phase concentration at site 2. The SSEs of the prediction of the model and the experimental data were minimized by the HYDRUS-1D code (Šimůnek et al., 2008) to optimize the sorption constant, the Langmuir component ( $Q_{\max} b$ ), the rate coefficient ( $\alpha$ ), and the fraction of equilibrium sites ( $f$ )

### 5.2.4 Parameter estimation

Water flow and solute transport in the soil columns can be treated as one-dimensional problem in mathematical simulations. The column was saturated with water and assumed to be homogeneously packed. A flux concentration boundary was assumed for the bottom of the column and a zero concentration gradient at the top or effluent of the column. The hydrodynamic dispersion coefficient  $D$  of the soil was estimated by curve fitting the bromide breakthrough curves (BTCs) with the nonlinear least-squares parameters optimization method (inverse model routine) of CXTFIT (CXTFIT; Toride et al., 1999). The solute transport parameters were initially estimated from bromide BTCs using CXTFIT by assuming equilibrium condition and

setting the retardation factor,  $R$  to 1. The two-region approach, assuming nonequilibrium conditions, was then applied to examine any physical nonequilibrium processes in the system. The hydrodynamic dispersion coefficient  $D$  obtained from the bromide BTC were then used to estimate the soil dispersivity,  $\lambda = D/v$ . The average dispersivity ( $\lambda_{avg}$ ) found from the bromide BTCs was used to estimate the sorption parameters of heavy metals under different conditions using linear and nonlinear sorption isotherm models as provided by *HYDRUS 1D* code version 4.Beta 1 (Šimůnek et al., 2008). In addition, chemical nonequilibrium model (2-site model, TSM) was used to estimate sorption parameters ( $Q_{max}$  and  $b$  in the case of Langmuir isotherm) and the nonequilibrium parameters ( $f$  and  $\alpha$ ) for transport of heavy metals. Least square errors were used to determine the appropriateness of the curve fitting. For the numerical calculations, the soil profile was discretized into 11 distributed nodes. The maximum time step for the simulation was chosen small enough  $\Delta t = 1$  hr to assure a mass balance error smaller than 1%.

## 5.3 Results and Discussion

### 5.3.1 Bromide Breakthrough Curves

The results of the nonequilibrium two-region model of the CXTFIT program for the bromide breakthrough curves are presented in Table 4.3. Since the model results gave  $\beta$  values equal 1 and  $\omega \geq 100$ , and when  $\omega \geq 10$ , the local equilibrium assumption appeared to be reasonably approximated (Bresseau et al., 1991). This suggests that all the water in the system was mobile (Toride et al., 1999). Consequently, equilibrium conditions can be assumed for the bromide data.

### 5.3.2 Heavy metal transport –experimental results

*Effect of concentration of secondary metals on their retention and retention of  $Pb^{2+}$*

Figures 5.1 – 5.3 show experimental BTCs of  $Pb^{2+}$  in single, binary and multi-metal systems at pH 5. Table 5.2 shows the properties of the columns used in heavy metal column studies. The column experiments with  $Pb^{2+}$  at 5 mM and  $Ni^{2+}$  at 3 mM and  $Pb^{2+}$  at 5 mM and  $Zn^{2+}$  at 10 mM were chosen for duplication since these two column experiments gave the lowest (~ 30% decrease) and highest (~ 60 % decrease)



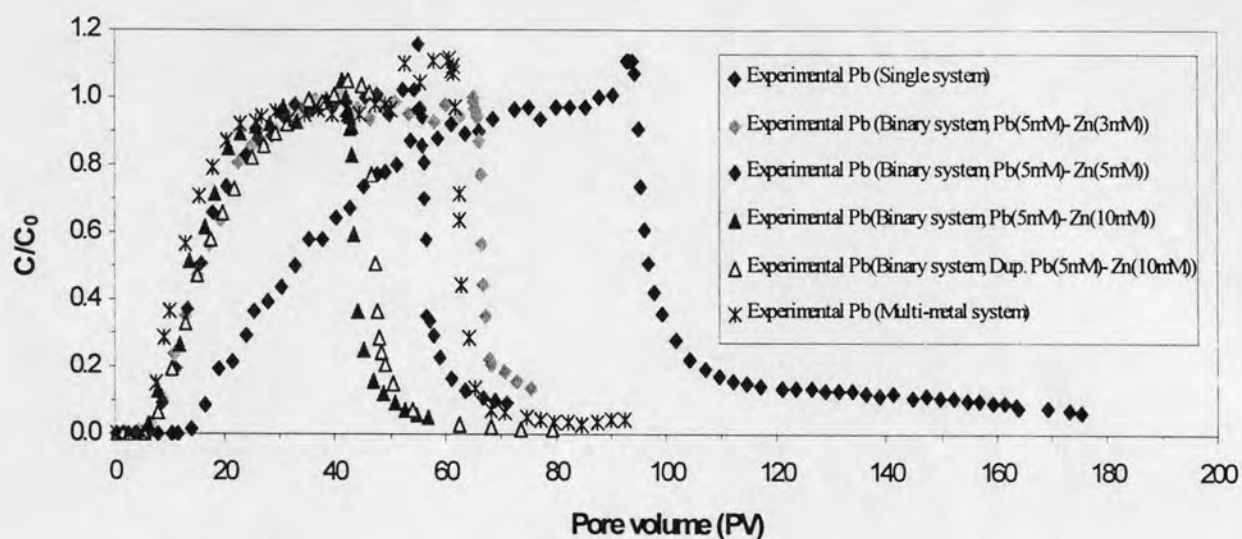


Figure 5.1 Effect of  $Zn^{2+}$  on  $Pb^{2+}$  retention onto lateritic soil at pH 5

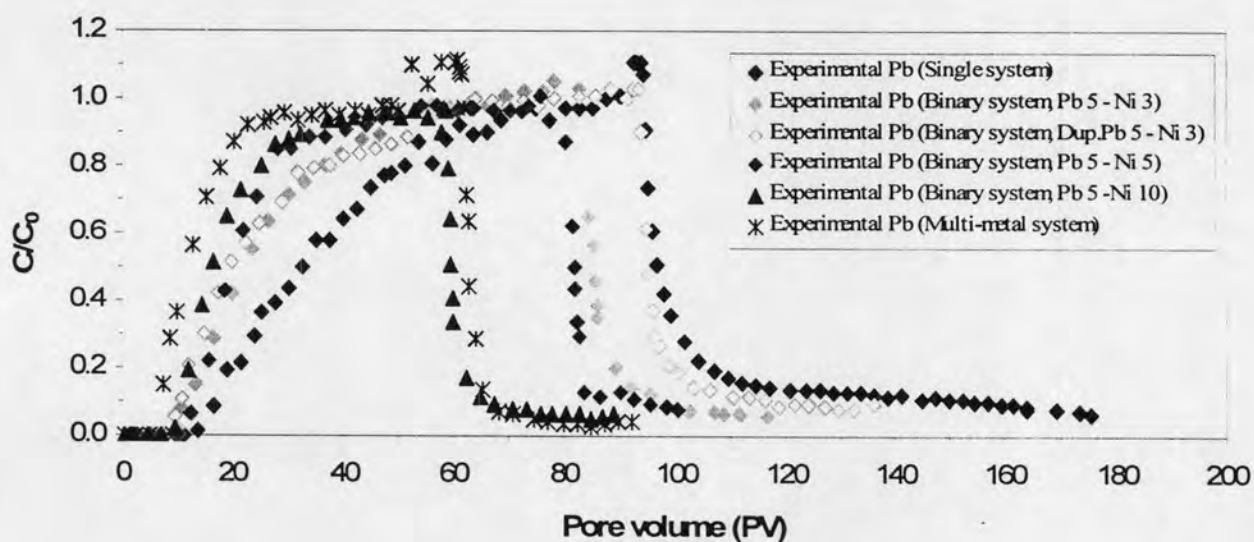


Figure 5.2 Effect of  $Ni^{2+}$  on  $Pb^{2+}$  retention onto lateritic soil at pH 5

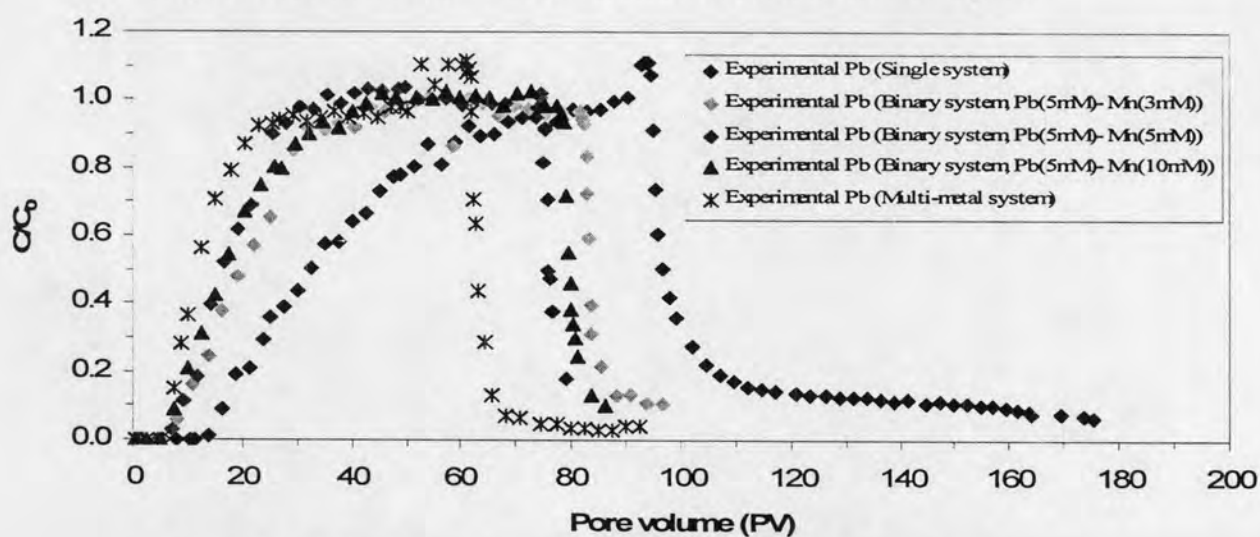


Figure 5.3 Effect of  $Mn^{2+}$  on  $Pb^{2+}$  retention onto lateritic soil at pH 5

**Table 5.2** Summary of parameters of the lateritic column studies with binary and multi-metal systems at 5.  $C_0$  initial concentration,  $L$  column length,  $\rho$  bulk density were determined experimentally,  $\eta$  porosity,  $q$  flow rate,  $v$  average pore-water velocity,  $R$  retardation factor,  $PV$  pore volume of the soil

System	$C_0$ (mM)		$L$ (cm)	$\rho$ (g cm <sup>-3</sup> )	$n$ (cm <sup>3</sup> cm <sup>-3</sup> )	$q$ (mL hr <sup>-1</sup> )	$v$ (cmhr <sup>-1</sup> )	$PV$	$R_{area}$ <sup>†</sup>		Sorbed/g soil(mM g <sup>-1</sup> )		mass recovery (%)	
	1 <sup>st</sup> metal (Pb <sup>2+</sup> )	2 <sup>nd</sup> metal							1 <sup>st</sup> metal (Pb <sup>2+</sup> )	2 <sup>nd</sup> metal	1 <sup>st</sup> metal (Pb <sup>2+</sup> )	2 <sup>nd</sup> metal	1 <sup>st</sup> metal (Pb <sup>2+</sup> )	2 <sup>nd</sup> metal
Pb <sup>2+</sup> -Ni <sup>2+</sup>	5.05*	0	10	1.03	0.62	7.76	2.55	31.5	35.35	-	0.117	-	73.45	-
	5.01 <sup>†</sup>	0	10	1.00	0.63	7.92	2.55	31.2	38.71	-	0.134	-	73.17	-
	4.86	3.01	10	1.00	0.63	8.45	2.72	31.5	25.53	17.68	0.082	0.037	78.03	86.64
	4.85 <sup>†</sup>	3.17	10	1.00	0.63	8.20	2.64	31.5	25.02	15.92	0.083	0.035	82.46	87.53
	4.93	5.13	10	1.04	0.62	8.21	2.71	32.1	22.74	13.77	0.076	0.048	76.88	87.18
	4.88	10.06	10	0.99	0.64	7.76	2.49	34.2	18.47	9.31	0.057	0.067	81.53	94.55
Pb <sup>2+</sup> -Zn <sup>2+</sup>	5.26	2.91	10	1.04	0.62	8.16	2.69	36.5	17.02	10.61	0.087	0.024	79.67	88.53
	5.22	5.36	10	1.04	0.62	8.19	2.71	36.4	16.81	9.50	0.067	0.039	79.97	91.91
	5.41	9.67	10	0.94	0.65	7.97	2.49	32.5	15.07	8.50	0.055	0.055	79.13	98.10
	4.33 <sup>†</sup>	9.48	10	0.92	0.66	7.63	2.35	29.9	17.41	9.61	0.056	0.068	72.45	93.11
Pb <sup>2+</sup> -Mn <sup>2+</sup>	5.31	2.73	10	1.04	0.62	8.58	2.84	30.5	20.90	13.92	0.079	0.024	81.12	88.99
	5.14	4.47	10	1.00	0.63	7.62	2.46	30.2	17.31	10.40	0.067	0.038	86.39	94.98
	4.85	8.66	10	1.02	0.62	8.28	2.70	32.3	16.98	8.52	0.057	0.066	86.48	94.12
Pb <sup>2+</sup> -Zn <sup>2+</sup> - Ni <sup>2+</sup> -Mn <sup>2+</sup>	4.56	Zn <sup>2+</sup> =4.73	10	0.94	0.65	8.33	2.60	32.5	13.68	8.10	0.047	0.028	86.18	96.58
		Ni <sup>2+</sup> =5.19								8.05		0.032		95.82
		Mn <sup>2+</sup> =4.38								6.95		0.023		100.03

umn derived from chapter 4; <sup>†</sup>Estimated from area method (Maraqa, 2001); <sup>‡</sup>Duplicated column

effects of the second metals ( $\text{Ni}^{2+}$  and  $\text{Zn}^{2+}$ ) on the retardation factors of  $\text{Pb}^{2+}$  (see Table 5.2). Over the experiment duration of about three weeks, a complete BTC of heavy metals was not achieved due to the extended tailing. It was observed from the BTCs that  $\text{Pb}^{2+}$  in a single metal system was sorbed more preferable by lateritic soil as the breakthrough times were longer than the BTCs in binary systems for different initial concentrations of secondary metals. For example, the initial breakthrough time for  $\text{Pb}^{2+}$  was about 9 pore volumes in  $\text{Pb}^{2+}$  (5 mM)-  $\text{Ni}^{2+}$  (3 mM) system while the breakthrough time was about 14 pore volumes in a single  $\text{Pb}^{2+}$  system (Figure 5.1). The BTCs of  $\text{Pb}^{2+}$  obtained in binary systems with increasing concentration of secondary metal and multi-metal system were found to be shorter than the BTCs of single  $\text{Pb}^{2+}$  system (Figures 5.1-5.3).

Another observation for binary systems was that the breakthrough times for secondary metals were earlier than that for  $\text{Pb}^{2+}$  (Figures 5.4 - 5.15). For example, the initial breakthrough time for  $\text{Ni}^{2+}$  was about 5 pore volume, which was less than the 9 PVs for  $\text{Pb}^{2+}$  in a  $\text{Pb}^{2+}$  (5 mM)-  $\text{Ni}^{2+}$  (3 mM) system (Figure 5.4).

One possible reason for the longer breakthrough times for  $\text{Pb}^{2+}$  is that  $\text{Pb}^{2+}$  has a smaller hydrated radius of 0.187 nm than  $\text{Ni}^{2+}$  (0.232 nm),  $\text{Zn}^{2+}$  (0.233 nm), and  $\text{Mn}^{2+}$  (0.235 nm) leading to higher coulombic or ionic forces of attraction of  $\text{Pb}^{2+}$  than the other metals. Hence,  $\text{Pb}^{2+}$  is more likely to be adsorbed as supported by the retardation factors of  $\text{Pb}^{2+}$ , obtained by the area method (Maraqa, 2001). Work done by Rodríguez-maroto et al. (2002) showed similar trends to this study where they found that the retention of  $\text{Pb}^{2+}$  was more preferable than  $\text{Cd}^{2+}$ , suggesting that the hydrated radius plays a role ( $\text{Cd}^{2+}$  hydrated radius is 0.23 nm which is larger than  $\text{Pb}^{2+}$ ). Due to the presence of metals in the system, the retardation factors of  $\text{Pb}^{2+}$  were lower (Table 5.2), for example, for the  $\text{Pb}^{2+}$ - $\text{Ni}^{2+}$  system with 3, 5, and 10 mM of  $\text{Ni}^{2+}$ , the retardation factors of  $\text{Pb}^{2+}$  changed from 37.03 in single metal system to 25.53 (~30% decrease), 22.74 (~40% decrease), and 18.74 (~50% decrease) for the different  $\text{Ni}^{2+}$  concentration, respectively. On the other hand, the retardation factors of  $\text{Ni}^{2+}$  decreased when the concentration of  $\text{Ni}^{2+}$  increased (i.e., 3 mM, 5 mM, and 10 mM), to 17.68 (~40% decrease), 13.77 (~50% decrease), and 9.31 (~70% decrease), respectively. These results were similar to Leitão and Zakharova (2003) who observed the absence of sorption of  $\text{Ni}^{2+}$  an initial concentration above 0.32 mM L<sup>-1</sup>



(for Sertã soil) and  $0.16 \text{ mM L}^{-1}$  (for Mortágue soil) and a decrease of retardation factors of  $\text{Zn}^{2+}$  in the presence of  $\text{Zn}^{2+}$ , and  $\text{Cu}^{2+}$  in column experiments. This is probably due to competition for sorption sites related to the presence of other two metals. Similarly, Bajracharya et al. (1996) found that the sorption coefficients of  $\text{Cd}^{2+}$  determined from column experiments was dependent on the influent concentration. With lower influent concentration, the sorption coefficient was higher. As seen in Table 5.2, the sorption capacity and retardation factors of  $\text{Pb}^{2+}$  reduced with increasing concentrations of secondary metals in both binary and multi-metal systems. However, no significant differences in retardation factors of  $\text{Pb}^{2+}$  were found for an increase in the concentrations of  $\text{Zn}^{2+}$  solution of more than 3 mM and concentration of  $\text{Mn}^{2+}$  of more than 5 mM in  $\text{Pb}^{2+}$ - $\text{Ni}^{2+}$  and  $\text{Pb}^{2+}$ - $\text{Mn}^{2+}$  systems, respectively. A probable reason is that  $\text{Pb}^{2+}$  was more preferably sorbed than  $\text{Zn}^{2+}$  and  $\text{Mn}^{2+}$  since the hydrated radius of  $\text{Pb}^{2+}$  (0.187 nm) was lower than of  $\text{Zn}^{2+}$  (0.233 nm) and  $\text{Mn}^{2+}$  (0.235). Consequently, the soil surface could be saturated with  $\text{Pb}^{2+}$ , resulting in limited  $\text{Zn}^{2+}$  and  $\text{Mn}^{2+}$  access to the sorption sites.

Mohan and Singh (2002) used batch studies to investigate the mutual effects of metals in the multi-metals system by measuring the ratio of the sorption capacity of one metal in multi-metals systems,  $q_i^{\text{mix}}$ , to the sorption capacity of given metal in single-metal system,  $q_i^0$ . If  $q_i^{\text{mix}}/q_i^0 > 1$ , sorption of metal  $i$  is enhanced by other metals ions. If  $q_i^{\text{mix}}/q_i^0 = 1$ , metals had no effects on each other. If  $q_i^{\text{mix}}/q_i^0 < 1$ , metal  $i$  competed with other metals for sorption sites of soil. In our study using the average sorption capacity as shown in Table 5.2, the values of  $q_i^{\text{mix}}/q_i^0$  were less than 1, indicating the competitive sorption of metals in binary and multi-metal systems. The batch studies conducted by Mohan and Chander (2006) showed competition of Fe with other metals (Mn, Zn, and Ca) for lignite sorption sites as evident by the  $q^{\text{mix}}/q^{\text{Fe}}$  being lower than 1. Similarly, Serrano et al. (2005) found that  $q^{\text{mix}}/q^{\text{Pb}}$  and  $q^{\text{mix}}/q^{\text{Cd}}$  were lower than 1, suggesting that the presence of  $\text{Pb}^{2+}$  and  $\text{Cd}^{2+}$  reduced sorption through competition for sorption sites on acid soils from Spain. In Table 5.2, sorption capacity of  $\text{Pb}^{2+}$  in the presence of secondary metals was reduced in comparison with that in the single component system. For example, the average sorption capacity of  $\text{Pb}^{2+}$  was about  $0.126 \text{ mM g}^{-1}$ , but this was reduced to 0.082 (~35% decrease), 0.076 (~40% decrease), and  $0.057 \text{ mM g}^{-1}$  (~55% decrease) when the  $\text{Ni}^{2+}$  solution were 3, 5, and 10 mM, respectively. On the other hand, the sorption capacity of  $\text{Ni}^{2+}$  was



reduced from approx.  $0.11 \text{ mM g}^{-1}$  (in single metal system) to  $0.048 \text{ mM g}^{-1}$  (~ 55% decrease) with the presence of  $\text{Pb}^{2+}$  at  $4.93 \text{ mM}$ . As described above, the reduction percentages of sorption capacity of  $\text{Pb}^{2+}$  were similar trend to the reductions of retardation factors. Furthermore, for a 1:1 molar ratio at  $5 \text{ mM}$  in binary systems, the presence of  $\text{Pb}^{2+}$  in the system reduced the sorption capacity of  $\text{Zn}^{2+}$  (~ 60 % decrease) which was the reduction for greater than other metals. Similarly, based on a 1:1 molar ratio in binary system, the percentage reduction of sorption capacity of  $\text{Pb}^{2+}$  (~ 40% for  $\text{Ni}^{2+}$ , 50% for  $\text{Zn}^{2+}$ , 50 % for  $\text{Mn}^{2+}$ ) caused by secondary metals were lower than those of secondary metals caused from  $\text{Pb}^{2+}$  (~ 50 % for  $\text{Ni}^{2+}$ , ~ 60 % for  $\text{Zn}^{2+}$ , 50 % for  $\text{Mn}^{2+}$ ).

For multi-metal system, the sorption capacity of  $\text{Pb}^{2+}$  was reduced from approx.  $0.13 \text{ mM g}^{-1}$  in single metal system to  $0.047 \text{ mM g}^{-1}$  (~60% decrease). On the other hand, the sorption capacities of  $\text{Zn}^{2+}$ ,  $\text{Ni}^{2+}$ , and  $\text{Mn}^{2+}$  were reduced from those in single metal systems to  $0.028$  (~70 % decrease),  $0.032$  (~70% decrease), and  $0.023$  (~60 % decrease)  $\text{mM g}^{-1}$ , respectively.  $\text{Pb}^{2+}$  caused the highest effect on the percentage reduction of sorption capacity of other metals. The preferred selectivity of one heavy metal ions over another is called selective sorption (Harter, 1992). The selectivity order is assumed to be inversely proportional to the hydrated radius of the metal with smaller radius being more favorable (Gomes et al., 2001). Thus, the expected order of selectivity is  $\text{Pb}^{2+}$  (0.187 nm radius) >  $\text{Ni}^{2+}$  (0.232 nm radius) >  $\text{Zn}^{2+}$  (0.233 nm radius) >  $\text{Mn}^{2+}$  (0.235 nm radius). As shown in the results, the sorption capacity in multi-metal system (under nearly the same initial concentration) were in the order:  $\text{Pb}^{2+}$  ( $0.047 \text{ mM g}^{-1}$ ) >  $\text{Ni}^{2+}$  ( $0.032 \text{ mM g}^{-1}$ ) >  $\text{Zn}^{2+}$  ( $0.028 \text{ mM g}^{-1}$ ) >  $\text{Mn}^{2+}$  ( $0.023 \text{ mM g}^{-1}$ ), which was in agreement with the order of selectivity of metals. Hence, the retardation factors follow the trend:  $\text{Pb}^{2+} > \text{Zn}^{2+} \sim \text{Ni}^{2+} > \text{Mn}^{2+}$  for multi-metal system. This would infer that the mobility of multi-metal through lateritic soil, would be in the order of  $\text{Mn}^{2+} > \text{Ni}^{2+} \sim \text{Zn}^{2+} > \text{Pb}^{2+}$ .

Interestingly, the data in Table 5.2 indicate that total sorption capacity of  $\text{Pb}^{2+}$  in single system, and the total sorption capacity of the metals in binary systems ( $\text{Pb}^{2+}$ - $\text{Ni}^{2+}$ ,  $\text{Pb}^{2+}$ - $\text{Zn}^{2+}$ ,  $\text{Pb}^{2+}$ - $\text{Mn}^{2+}$ ), and in a multi-metal system for equal molar concentration system were approx. 0.13, 0.12, 0.11, 0.11, and  $0.13 \text{ mM g}^{-1}$ ,

respectively (addition of column 12+13). This indicates that the maximum sorption capacity of lateritic soil was approx.  $0.13 \text{ mM g}^{-1}$ .

As mentioned above, the presence of secondary metal ions in the systems, resulted in a decrease in the sorption capacity and retardation factors of the primary metal ( $\text{Pb}^{2+}$ ), indicating there was competitive sorption among metals for the available sorption site on the lateritic soil. As more metal ions were presented in the system, the competition among metal ions for available sites was more obvious.

### 5.3.3 Heavy metal transport modeling

The breakthrough curves of heavy metals were fitted using the equilibrium convection-dispersion model ( $CD_{eq}$ ) and nonequilibrium model (Two-site model,  $TSM$ ) of *HYDRUS-1D*. A limitation of this model is that the model could not represent the interaction between solutes in the system. Thus, each BTC was fitted individually. The model-simulated curves derived from the models are presented in Figures 5.4 - 5.15 and the fitted parameters are presented in Tables 5.3 and 5.4. For comparison purposes, the experimental data for  $\text{Pb}^{2+}$  BTC in a single system were presented along with  $\text{Pb}^{2+}$  in binary and multi-metal systems in Figures 5.4 - 5.15. For the same initial concentrations of secondary metals ( $\text{Ni}^{2+}$ ,  $\text{Zn}^{2+}$ , and  $\text{Mn}^{2+}$ ) at 5 mM, the observed BTCs of these metals in single systems were plotted in Figures 5.6, 5.9, 5.12, 5.15 to compare with the BTCs of such metals in binary and multi-metal systems.

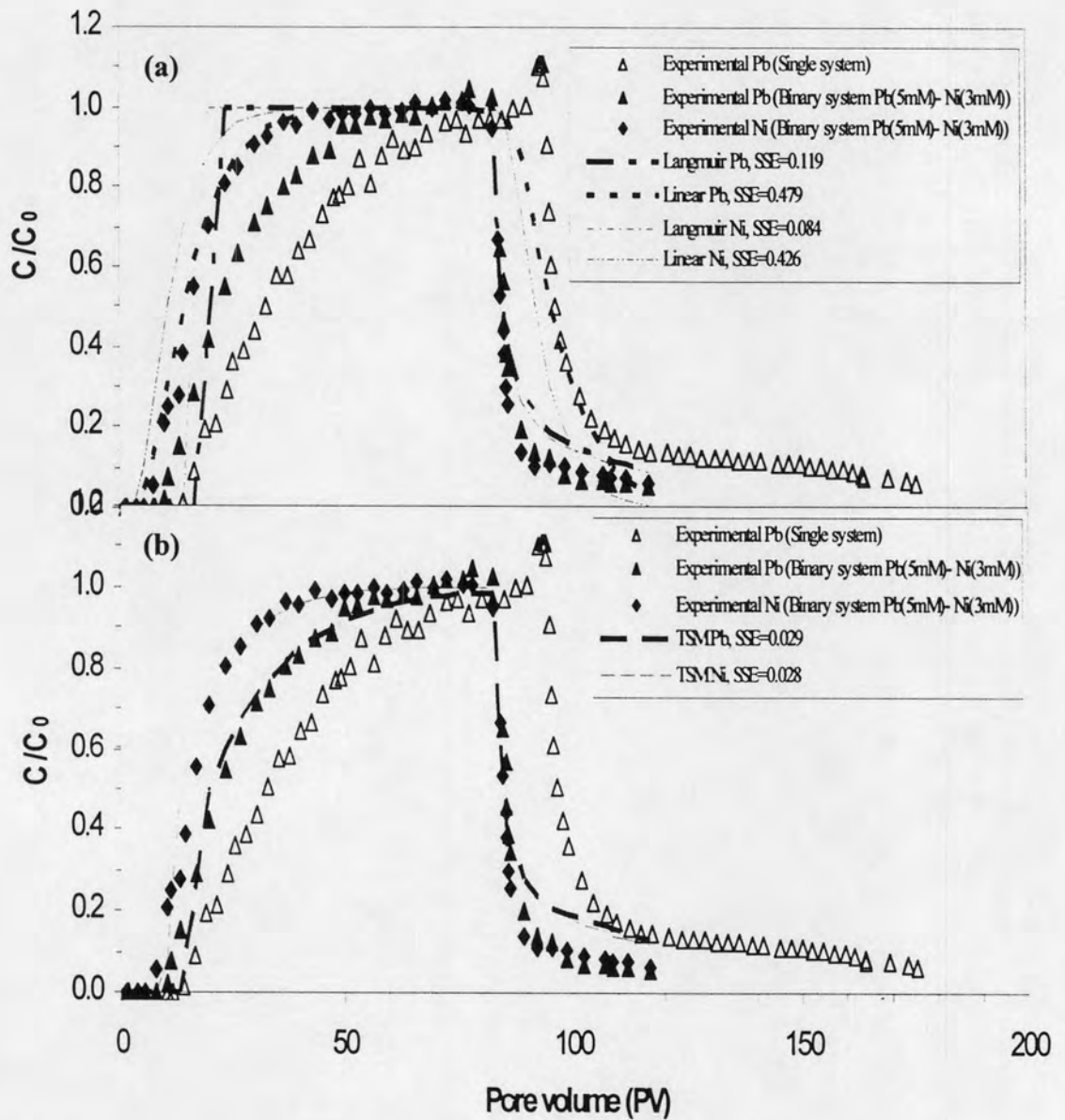


**Figure 5.4** Heavy metal breakthrough data in lateritic soil column for  $Pb^{2+}$  (5 mM) and  $Pb^{2+}$  (5 mM)-  $Ni^{2+}$  (3 mM) at pH 5 and different model fits (a) equilibrium convection-dispersion model ( $CD_{eq}$ ) with linear and Langmuir isotherm, (b) Two-site model (TSM)

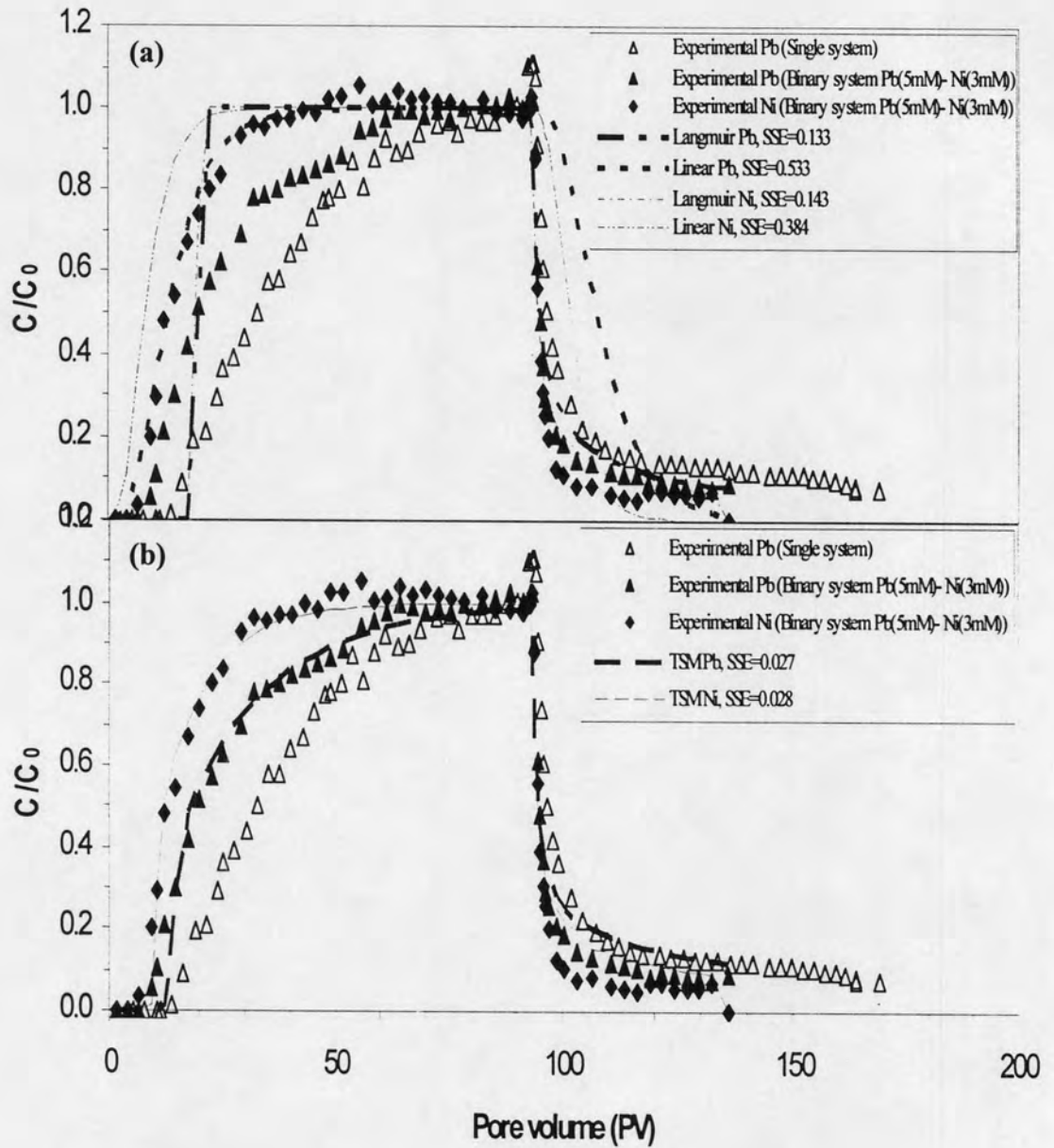


**Figure 5.5** Heavy metal breakthrough data in lateritic soil column for  $\text{Pb}^{2+}$  (5 mM) and  $\text{Pb}^{2+}$  (5 mM)-  $\text{Ni}^{2+}$  (3 mM) (duplicated column) at pH 5 and different model fits (a) the equilibrium convection-dispersion model ( $\text{CD}_{\text{eq}}$ ) with linear and Langmuir isotherm, (b) Two-site model (TSM)



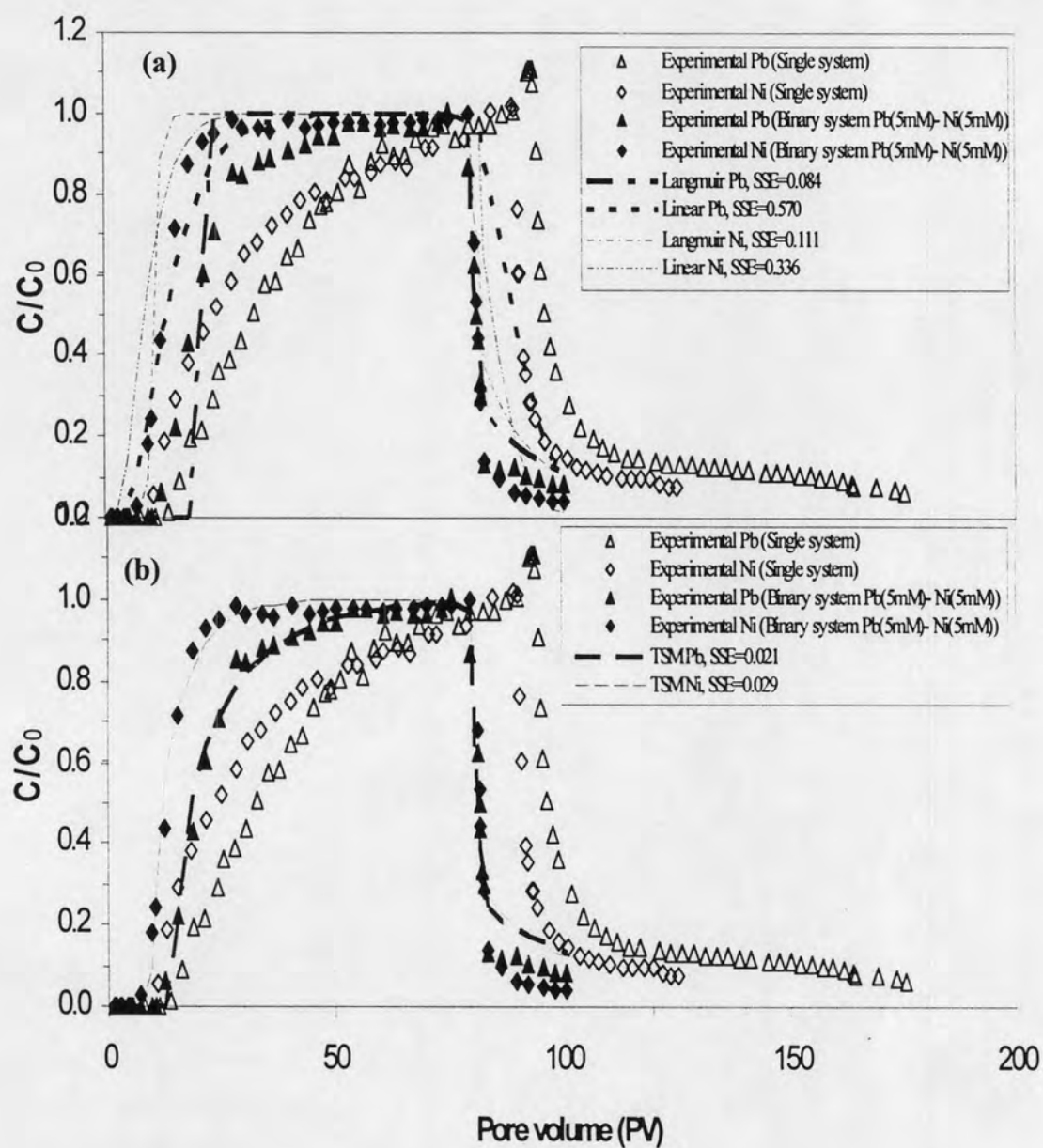


**Figure 5.6** Heavy metal breakthrough data in lateritic soil column for  $\text{Pb}^{2+}$  (5 mM),  $\text{Ni}^{2+}$  (5 mM), and  $\text{Pb}^{2+}$  (5 mM)-  $\text{Ni}^{2+}$  (5 mM) at pH 5 and different fits (a) the equilibrium convection-dispersion model ( $\text{CD}_{\text{eq}}$ ) with linear and Langmuir isotherm, (b) Two-site model (TSM)

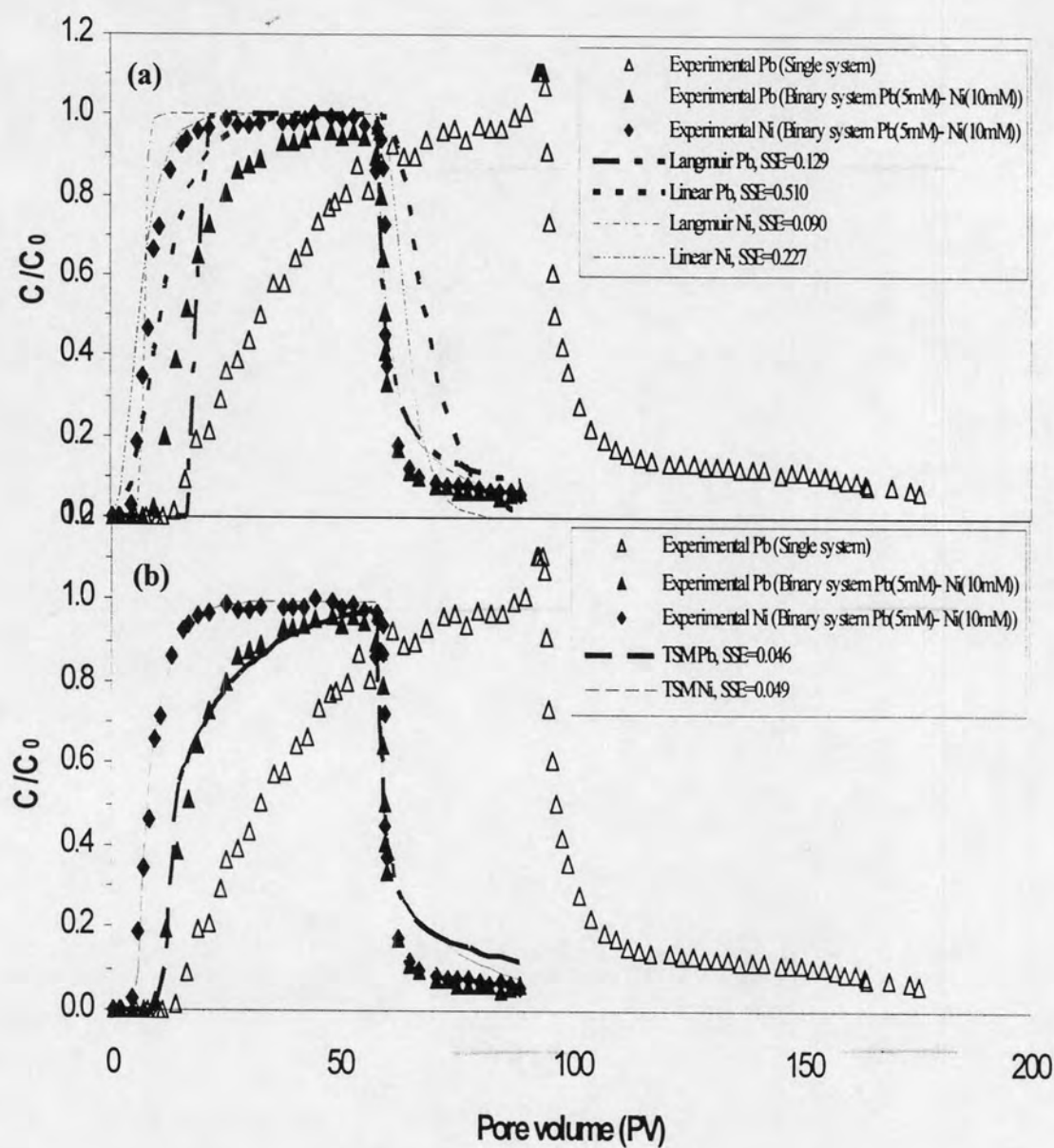


**Figure 5.7** Heavy metal breakthrough data in lateritic soil column for  $Pb^{2+}$  (5 mM) and  $Pb^{2+}$  (5 mM)-  $Ni^{2+}$  (10 mM) at pH 5 and different model fits (a) the equilibrium convection-dispersion model ( $CD_{eq}$ ) with linear and Langmuir isotherm, (b) Two-site model (TSM)

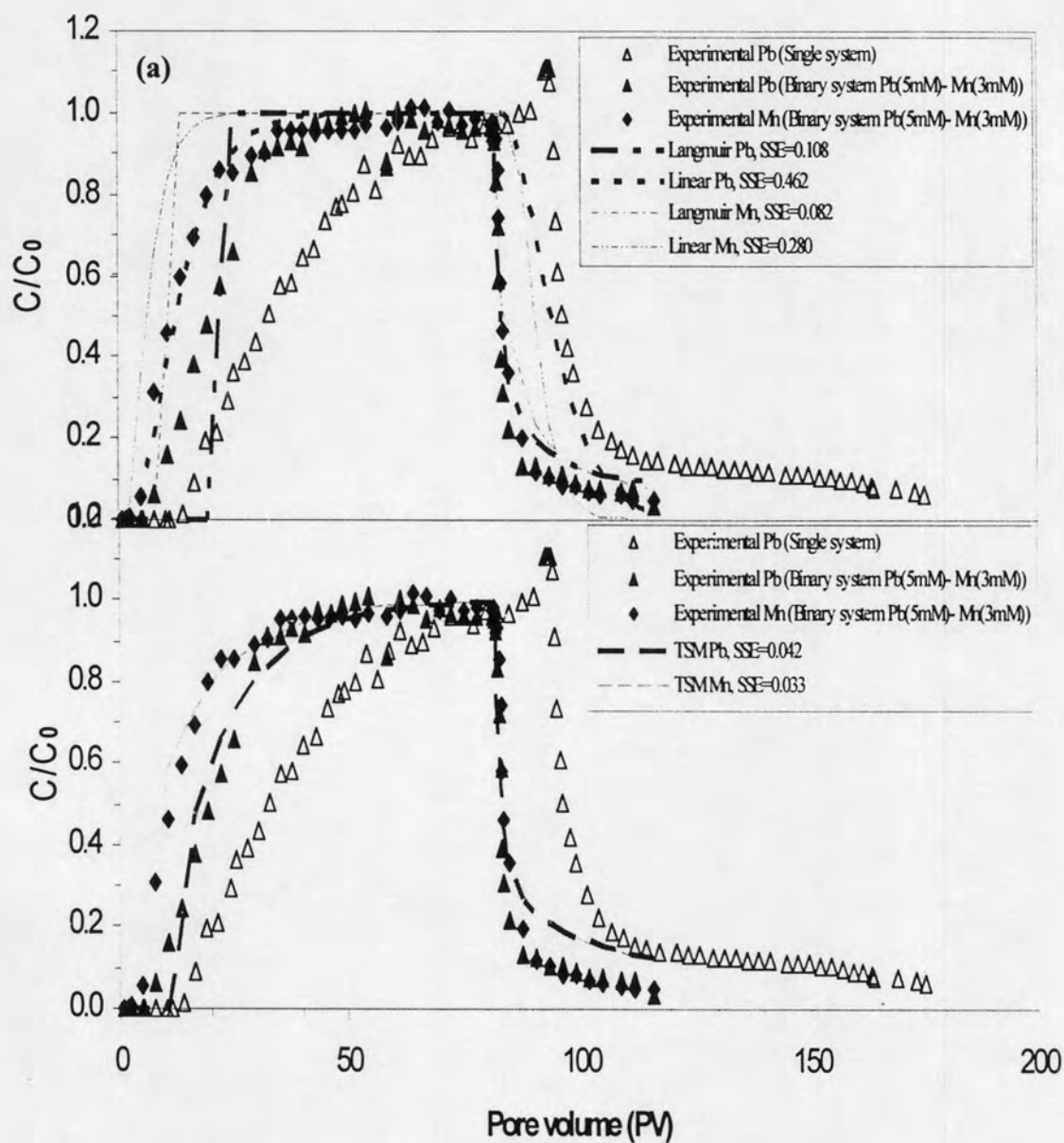


**Figure 5.8** Heavy metal breakthrough data in lateritic soil column for  $\text{Pb}^{2+}$  (5 mM) and  $\text{Pb}^{2+}$  (5 mM)-  $\text{Mn}^{2+}$  (3 mM) at pH 5 and different model fits (a) the equilibrium convection-dispersion model ( $\text{CD}_{\text{eq}}$ ) with linear and Langmuir isotherm (b) Two-site model (TSM)

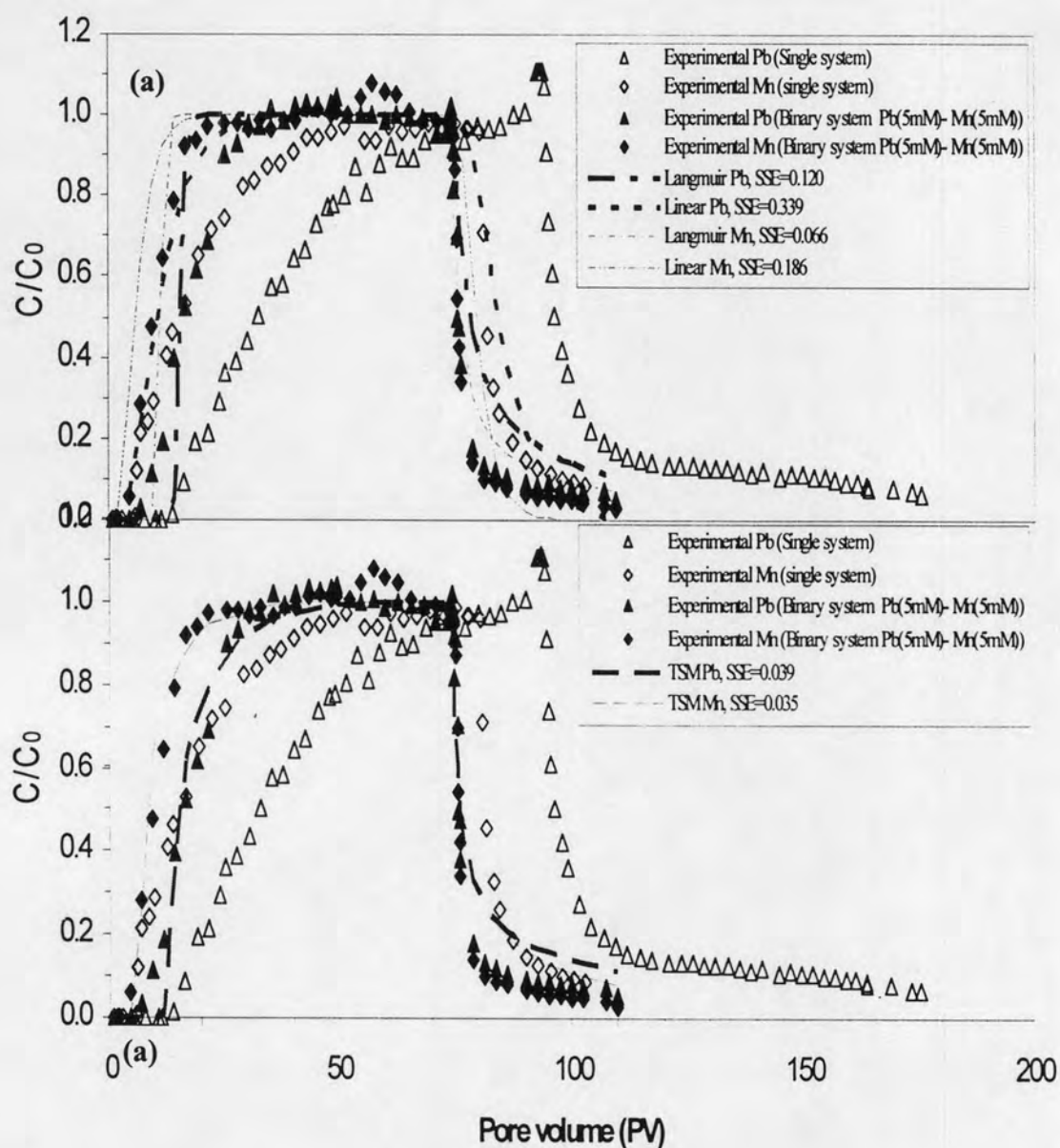


**Figure 5.9** Heavy metal breakthrough data in lateritic soil column for  $\text{Pb}^{2+}$  (5 mM),  $\text{Mn}^{2+}$  (5 mM), and  $\text{Pb}^{2+}$  (5 mM) -  $\text{Mn}^{2+}$  (5 mM) at pH 5 and different model fits (a) the equilibrium convection-dispersion model ( $\text{CD}_{\text{eq}}$ ) with linear and Langmuir isotherm (b) Two-site model (TSM)



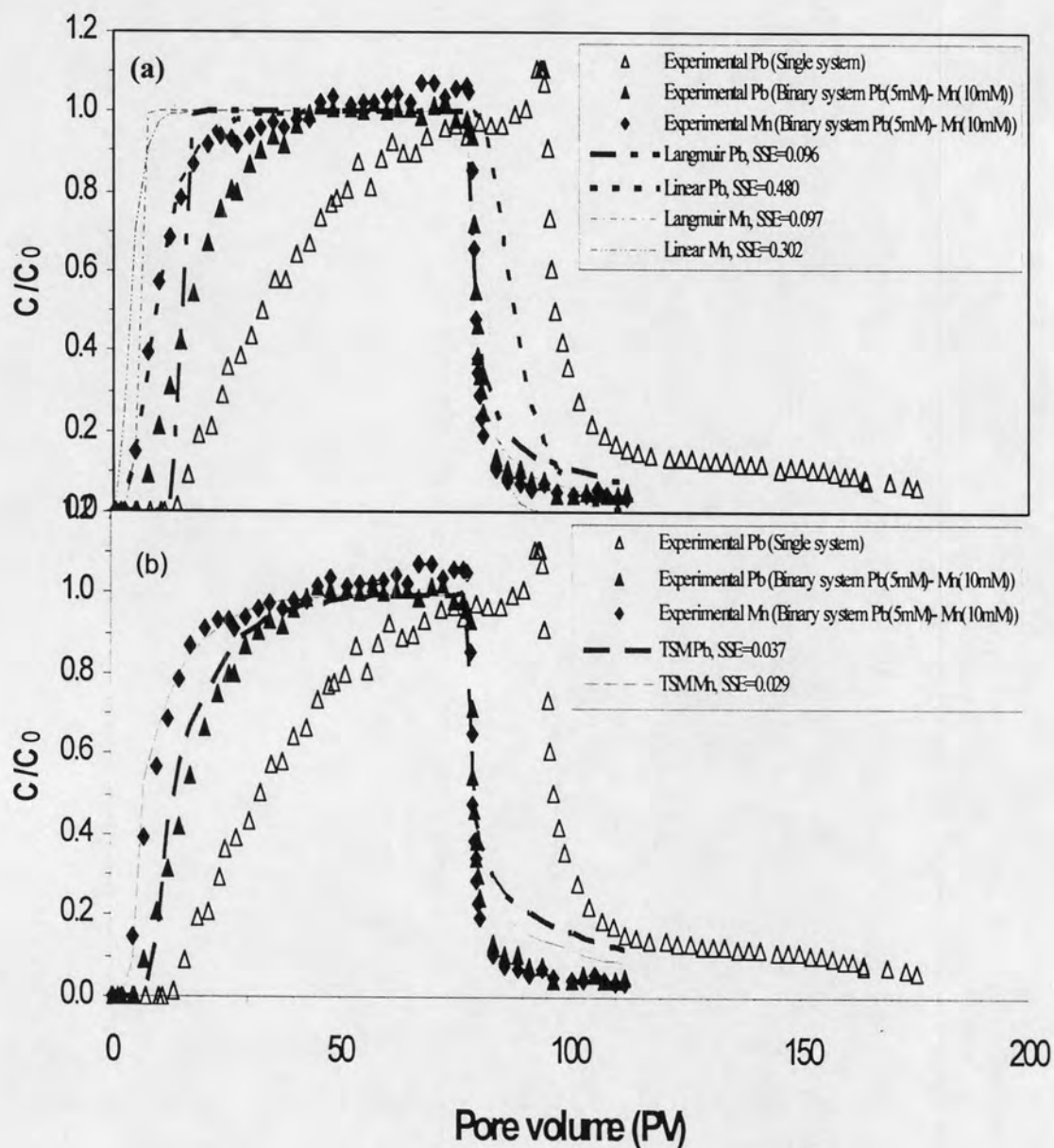


**Figure 5.10** Heavy metal breakthrough data in lateritic soil column for  $\text{Pb}^{2+}$  (5 mM) and  $\text{Pb}^{2+}$  (5 mM)-  $\text{Mn}^{2+}$  (10 mM) at pH 5 and different model fits (a) the equilibrium convection-dispersion model ( $\text{CD}_{\text{eq}}$ ) with linear and Langmuir isotherm (b) Two-site model (TSM)

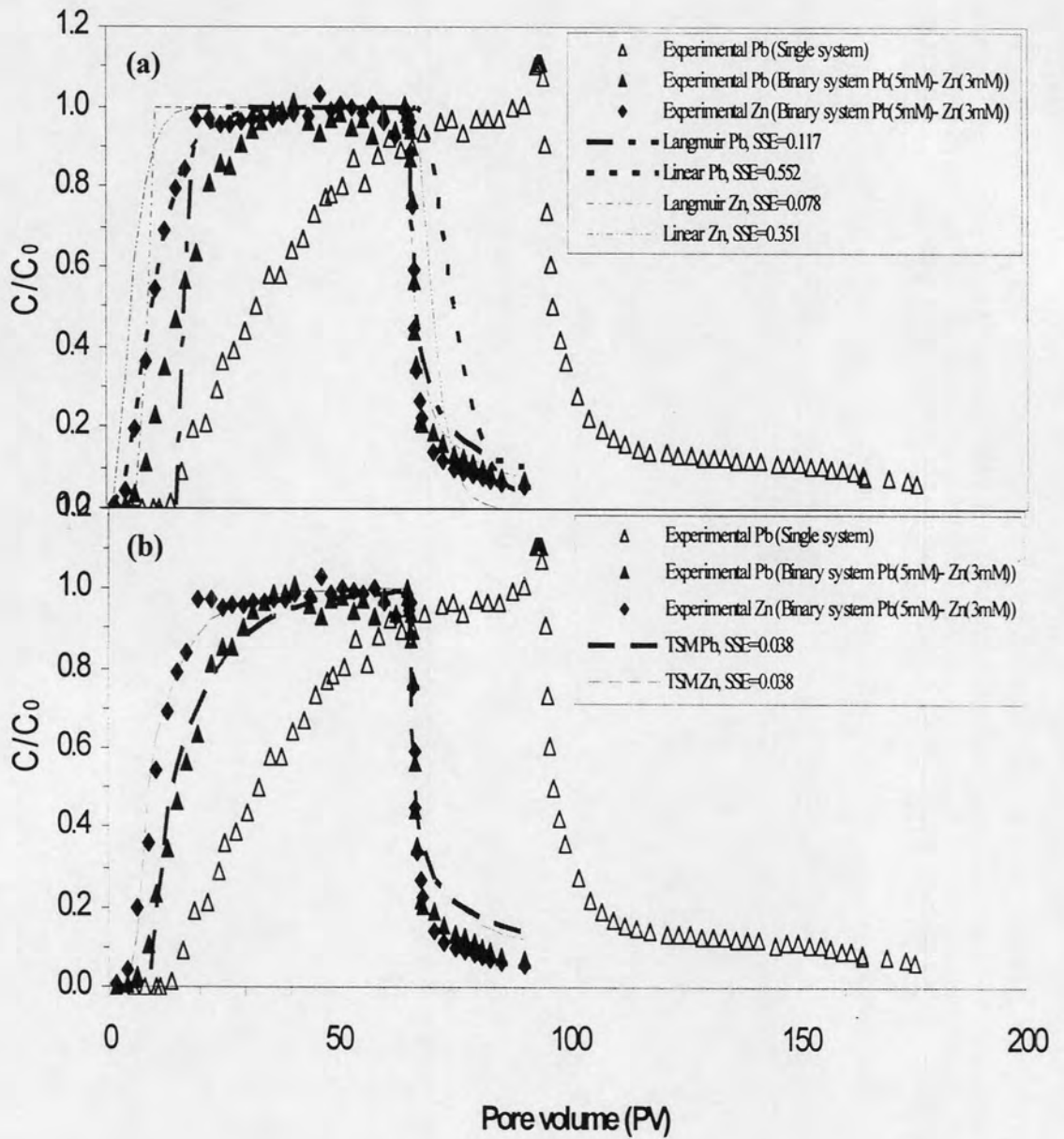


**Figure 5.11** Heavy metal breakthrough data in lateritic soil column for  $Pb^{2+}$  (5 mM) and  $Pb^{2+}$  (5 mM)-  $Zn^{2+}$  (3 mM) at pH 5 and different model fits (a) the equilibrium convection-dispersion model ( $CD_{eq}$ ) with linear and Langmuir isotherm (b) Two-site model (TSM)

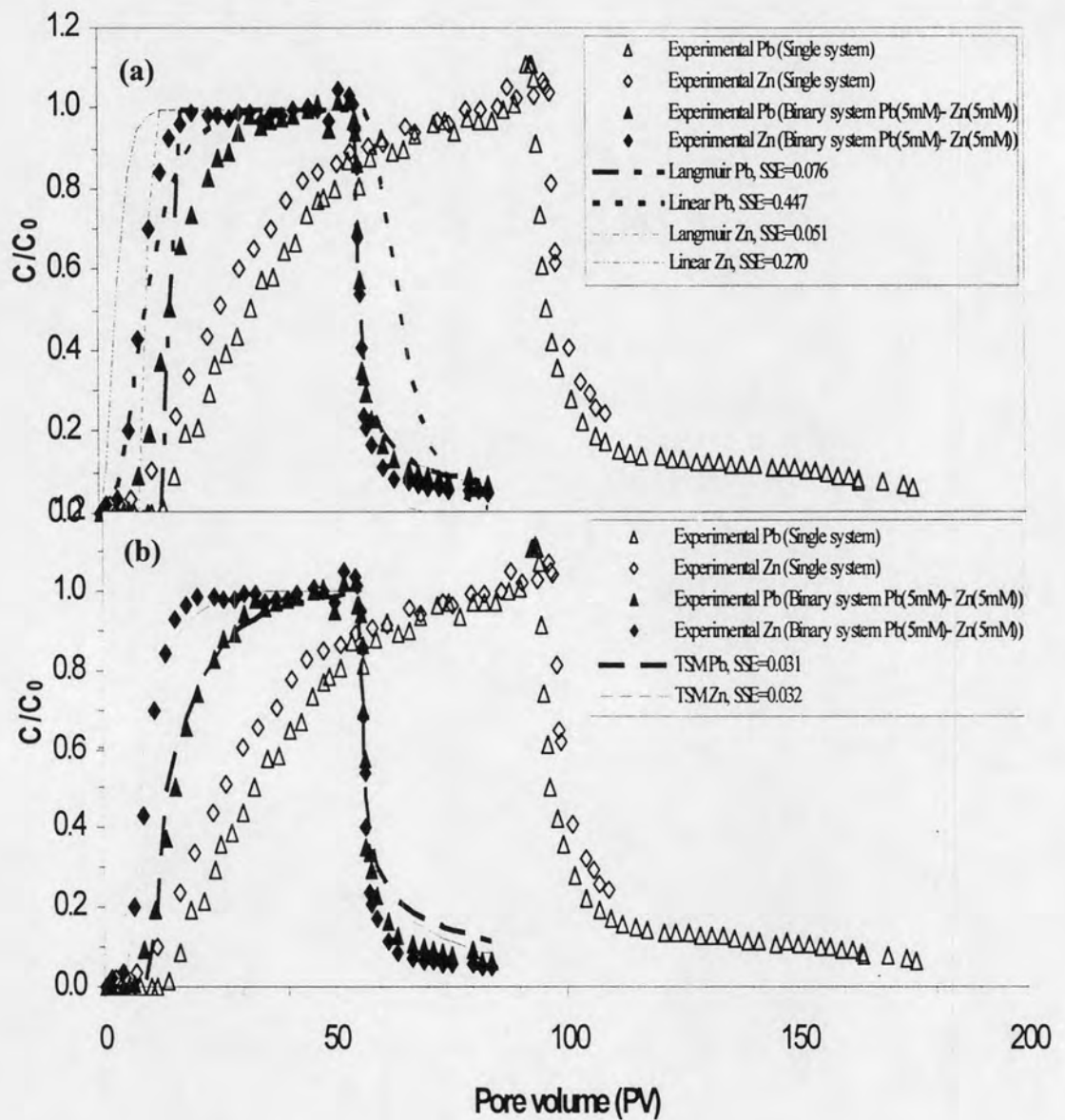


**Figure 5.12** Heavy metal breakthrough data in lateritic soil column for  $Pb^{2+}$  (5 mM),  $Zn^{2+}$  (5 mM) and  $Pb^{2+}$  (5 mM)-  $Zn^{2+}$  (5 mM) at pH 5 and different model fits (a) the equilibrium convection-dispersion model ( $CD_{eq}$ ) with linear and Langmuir isotherm (b) Two-site model (TSM)

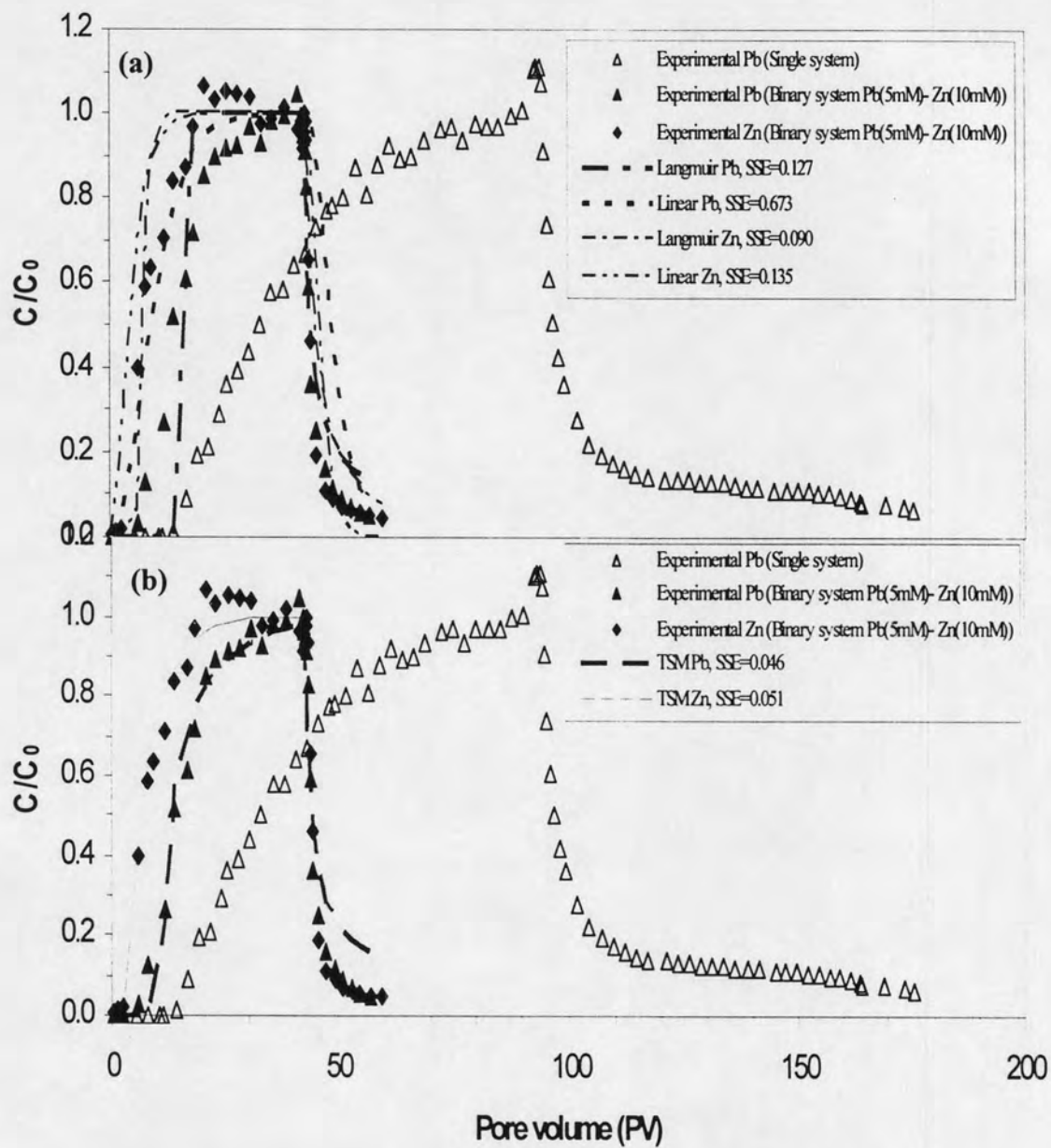


**Figure 5.13** Heavy metal breakthrough data in lateritic soil column for  $\text{Pb}^{2+}$  (5 mM) and  $\text{Pb}^{2+}$  (5 mM)-  $\text{Zn}^{2+}$  (10 mM) at pH 5 and different model fits (a) the equilibrium convection-dispersion model ( $\text{CD}_{\text{eq}}$ ) with linear and Langmuir isotherm (b) Two-site model (TSM)



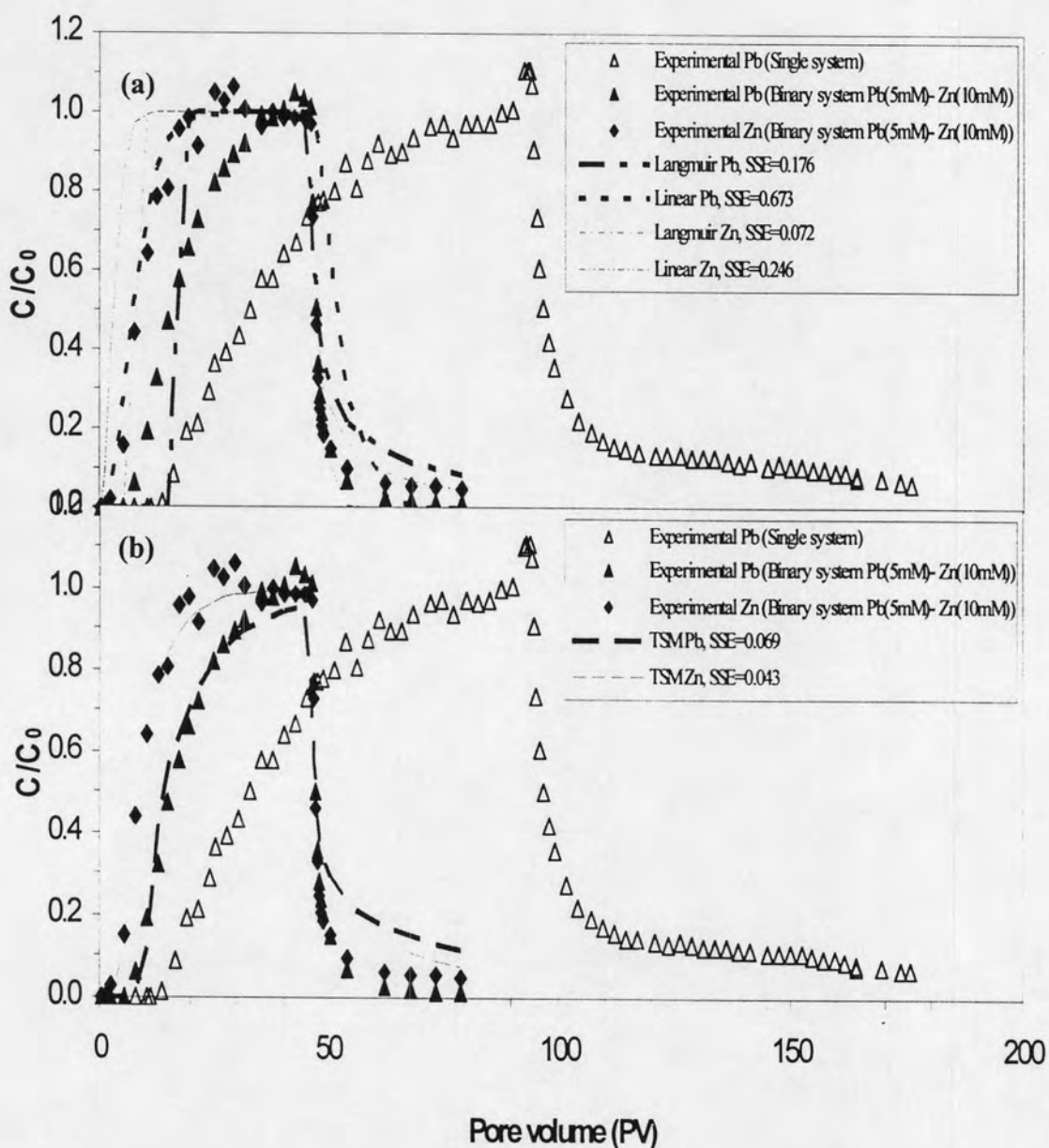


**Figure 5.14** Heavy metal breakthrough data in lateritic soil column for  $Pb^{2+}$  (5 mM) and  $Pb^{2+}$  (5 mM)- $Zn^{2+}$  (10 mM) (Duplicated column) at pH 5 and different model fits (a) the equilibrium convection-dispersion model ( $CD_{eq}$ ) with linear and Langmuir isotherm (b) Two-site model (TSM)

### 5.3.3.1 Equilibrium convection-dispersion model ( $CD_{eq}$ )

The equilibrium model is based on the local equilibrium assumption (*LEA*) where sorption is assumed to be fast relative to pore-water velocity. Both linear and nonlinear isotherm (Langmuir) were used in the equilibrium model to curve fit the metal BTCs as shown Figures 5.4 (a) - 5.15 (a). Table 5.3 presents the estimated parameters derived from *HYDRUS-1D* by minimizing the sum of square errors (SSE). As shown in Table 5.3, the SSE showed that the Langmuir isotherm explained the experimental data better than the linear isotherm. With linear sorption isotherm, the initial breakthrough time of the best fit curve was less than the experimental data and the number of pore volumes at which the effluent concentration was equal to that of influent ( $C_e = C_0$ ) were faster than those of the experimental BTCs. Moreover, the rising and decreasing limbs derived from the linear model were overestimated when compared with the experimental data (Figures 5.4 (a) - 5.15 (a)).

As shown in Figures 5.4 to 5.15, a characteristic aspect of the experimental BTCs in binary and multi-metal systems was the asymmetrical shape with a sharply rising front and a relatively more dispersed elution portion, suggesting nonlinear sorption behavior. The BTCs for this study are similar to the work of Yolcubal and Akyol (2007) for column studies of Cr(VI) in calcareous Karst soil, where the breakthrough curves of Cr(VI) were asymmetrical with a sharply rising front and a more dispersed portion. The experimental BTCs were better described by Langmuir-isotherm than those fitted with linear isotherm giving lower values of *SSE* (Table 5.3). Although the BTCs obtained with Langmuir isotherm fitted better than those using linear isotherm, the Langmuir-isotherm-simulated BTCs showed sharp concentration fronts, and did not fit well with all observed data, especially the rising limb portion (Figures 5.4 (a) – 5.15 (a)). In addition, the Langmuir-isotherm-simulated BTCs could not describe the experimental BTCs well as the predicted initial breakthrough times were more than the experimental breakthrough times for metals in individual systems. As observed by others, the asymmetrical shape of metal BTCs with long tailings may be better described by a nonequilibrium transport model (Pang et al., 2002; Tsang and Lo, 2006).

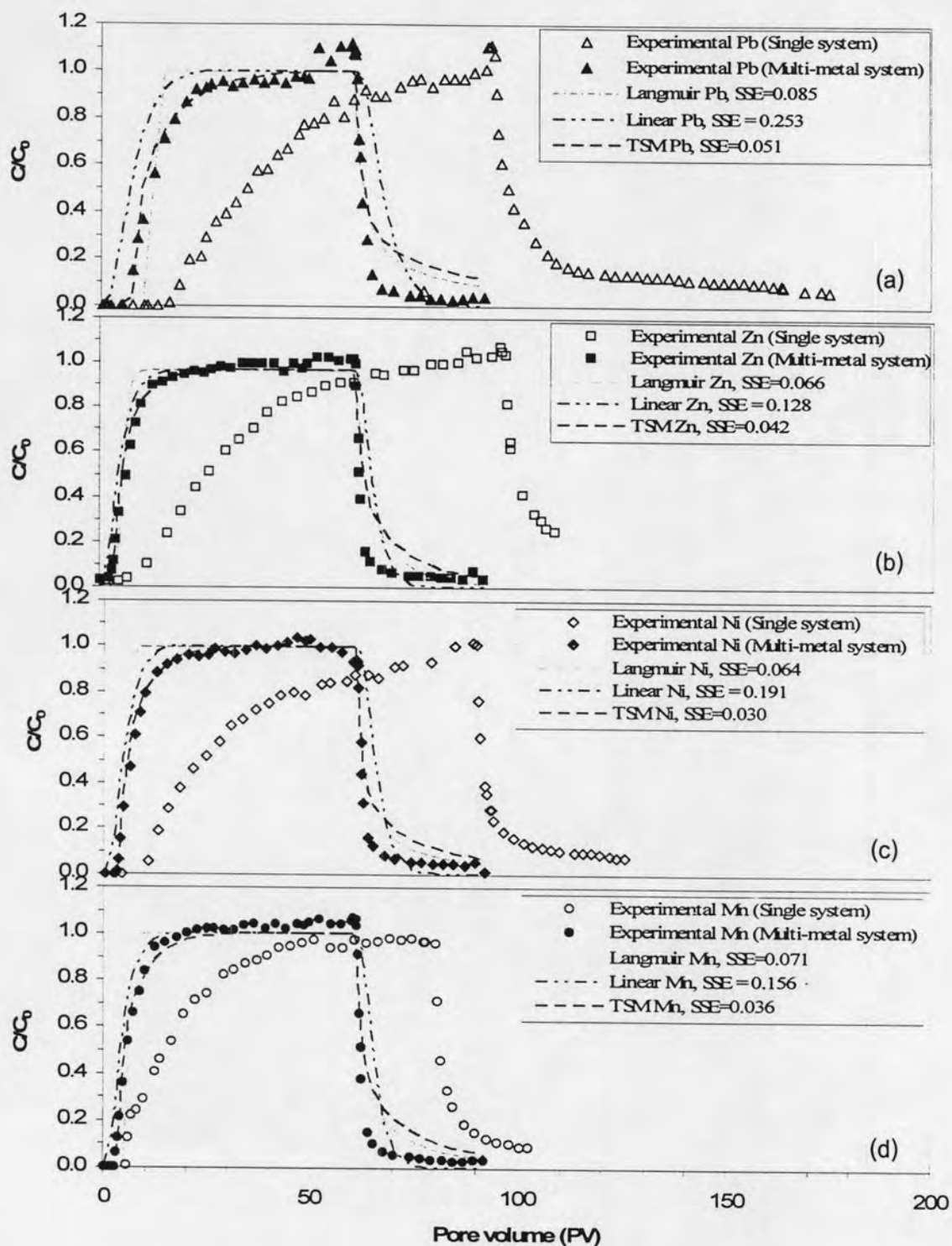


**Figure 5.15** Heavy metal breakthrough data in lateritic soil column for multi-metal system ( $\text{Pb}^{2+}$  5 mM-  $\text{Zn}^{2+}$  5 mM-  $\text{Ni}^{2+}$  mM-  $\text{Mn}^{2+}$  5 mM) at pH 5 and different fits with the equilibrium convection-dispersion model ( $\text{CD}_{\text{eq}}$ ) with linear and Langmuir isotherm and Two-site model (TSM) were compared with observed data in single and binary system: (a)  $\text{Pb}^{2+}$ , (b)  $\text{Zn}^{2+}$ , (c)  $\text{Ni}^{2+}$ , and (d)  $\text{Mn}^{2+}$

### 5.3.3.2 Chemical nonequilibrium model (Two-site model, TSM)

The equilibrium convection-dispersion model using linear and Langmuir sorption isotherm did not fully described the heavy metal BTCs in lateritic soil as shown in Figures 5.4 (a) - 5.15 (a). Characteristics of nonequilibrium sorption-related transport have been observed for some metals in repacked soil and/or gravel column (Tsang and Lo, 2006 Pang et al., 2002). One of the approaches in describing non-equilibrium transport is to assume a short, initial fast phase of sorption followed by an extended period of slower sorption (Sparks, 1995). This process can be modeled using the two-site sorption model (TSM). The BTCs were fitted with this model as shown in Figures 5.4 (b) - 5.15 (b). Two-site model (TSM) could describe all of heavy metal BTCs better than linear and Langmuir model based on local equilibrium. For example, SSE derived from fitting BTC of  $Pb^{2+}$  in  $Pb^{2+}$  (5 Mm) -  $Ni^{2+}$  (3 mM) system at pH 5 were:  $SSE_{TSM}$  (0.029) <  $SSE_{Langmuir}$  (0.119) <  $SSE_{Linear}$  (0.479). These results were similar to the work done by others. For example Kookana et al. (1994) observed asymmetrical BTCs for Cd in Spodosol and Oxisol soil which may be due to sorption-related (chemical) nonequilibrium behavior. Another study by Pang et al. (2002), on the effects of pore-water velocity on chemical nonequilibrium of single metal systems of Cd, Zn, and Pb through alluvial gravel columns showed that the BTCs of each metals can be fitted using the two-site model. According to column studies with different secondary metals in this study, the TSM fitted the rising and the declining limb of the breakthrough curves of heavy metals (Figures 5.4 (b) - 5.15 (b)) better than the equilibrium assumption. Applying the *t*-test on the average SSEs obtained from the chemical nonequilibrium two-site model and the convection-dispersion model with Langmuir isotherm for individual metals in binary and multi-metal systems, it was found that the curve-fitted results of the chemical non-equilibrium two-site model were significantly different from the equilibrium convection-dispersion model for pH 4 and 5 (*t*-test,  $P < 0.05$ ), indicating that the fitted values by chemical nonequilibrium two-site model presented a better agreement with the experimental results (statistically significant,  $P < 0.05$ ) than the equilibrium convection-dispersion model (see Appendix D).

For the sake of comparison, according to the best fit parameters from the two-site model (TSM), the maximum sorption capacity of  $Pb^{2+}$ ,  $(Q_{max})_{Pb^{2+}}$ , in the



single system had the highest sorption capacity than to those in the binary and multiple metal systems (Figures 5.16), which is in agreement with the retardation factors and average sorption capacity of  $Pb^{2+}$  in single system over those in binary and multi-metal systems as mentioned in the section 5.3.2. Figure 5.16 plots the  $(Q_{max})_{Pb^{2+}}$  from the TSM versus the concentrations of the secondary metals. With increasing concentrations of the secondary metals in binary and multi-metal systems, the maximum sorption capacity of  $Pb^{2+}$ ,  $(Q_{max})_{Pb^{2+}}$ , decreased with respect to the maximum sorption capacity of  $Pb^{2+}$  in the single system. For example, in  $Pb^{2+}$ - $Zn^{2+}$  system, the maximum sorption capacity of  $Pb^{2+}$  for 0 mM  $Zn^{2+}$  statistically different than the maximum sorption capacity of  $Pb^{2+}$  for 3 mM of  $Zn^{2+}$ . When the concentration of  $Zn^{2+}$  was more than 3 mM, the maximum sorption capacity of  $Pb^{2+}$  showed decreasing trend but was not significantly different from the maximum sorption capacities of higher  $Zn^{2+}$  concentration. This was in agreement with decreasing retardation factors of  $Pb^{2+}$  as affected by concentration of  $Zn^{2+}$  as mentioned in section 5.3.2.

The fraction of the instantaneous equilibrium site ( $f$ ) of all metals for the lateritic soil was consistently in the range of 30 to 58 % of the total sorption sites for both binary and multi-metal system which was similar to that of the instantaneous site in single metal system. Since each metal in binary and multi-metal systems was fitted individually, the fractions of the instantaneous site of 1<sup>st</sup> and 2<sup>nd</sup> metal of each system derived from modeling were expected to be in the same range (Table 5.3). The fairly similar fraction of the instantaneous sites for single and binary system is in agreement with the study by Schwarzenbach and Westall (1981), which indicated that the fraction of instantaneous site ( $f$ ) would be dependent on pore velocity for a chemical nonequilibrium process. Therefore, under similar pore velocity conditions in this study for single or binary system, the fraction simultaneous sorption site ( $f$ ) should be similar.

The TSM correctly explained the early tailing of the asymmetrical portion of heavy metal BTCs under both binary and multi-metal systems (Figure 5.4 (b) -5.15 (b)), but slightly overestimated the extended tailing of heavy metals. This was probably due to the rate of sorption/desorption which could not be described by a first-order rate constant (Connaughton et al., 1993; Selim, 1999) or more than one

type of kinetic rates are needed in addition to the instantaneous sorption sites. Selim (1999) observed that the sorption/desorption behavior of  $\text{Cu}^{2+}$  for a McLaren soil showed hysteresis behavior or nonsingularity at high concentration, indicating this behavior could not be explained using first-order rate constant. Drillia (2005) found that soil with little organic matter, but with strong sorption hysteresis, might be described by a slower reversible or even an irreversible process that is not included in two-site model used in this study. In addition, the extended tailings might be controlled by mass transfer diffusion that was not accounted for in the two-site model, (Beigel and Pietro, 1999). Since the column studies do not provide information on hysteresis and/or mass transfer, further separate experimentation are required to more precisely model and predict of heavy metals transport through this soil (Seuntjens et al., 2001; Pang et al., 2002).

**Table 5.3** Estimated transport parameters for heavy metal breakthrough curves using linear and Langmuir isotherm from equilibrium convection-dispersion approaches generated by HYDRUS-1D

No	System	$C_0$ (mM)		$\lambda^*$ (cm)	Measured $v$ (cm hr <sup>-1</sup> )	Equilibrium model fit									
		1 <sup>st</sup> metal (Pb <sup>2+</sup> )	2 <sup>nd</sup> metal			1 <sup>st</sup> metal					2 <sup>nd</sup> metal				
						Linear		Langmuir			Linear		Langmuir		
						$K_d \pm 95\%CI$ (L g <sup>-1</sup> )	SSE	$Q_{max} \pm 95\%CI$ (mM g <sup>-1</sup> )	$b \pm 95\%CI$ (L mM <sup>-1</sup> )	SSE	$K_d \pm 95\%CI$ (L g <sup>-1</sup> )	SSE	$Q_{max} \pm 95\%CI$ (mM g <sup>-1</sup> )	$b \pm 95\%CI$ (L mM <sup>-1</sup> )	SSE
1		5.05*	0	1.42	2.55	20.40±0.04	0.43	0.17±0.01	10.75±0.21	0.15	-	-	-	-	-
2		5.01*	0	0.97	2.55	24.53±0.01	0.77	0.16±0.07	6.09±2.42	0.10	-	-	-	-	-
3	Pb <sup>2+</sup> -Ni <sup>2+</sup>	4.86	3.01	1.42	2.72	15.34±0.01	0.48	0.10±0.06	5.09±2.41	0.12	11.34±0.01	0.43	0.05±0.01	7.25±1.84	0.08
4		4.85 <sup>†</sup>	3.17	1.57	2.82	15.14±0.01	0.53	0.11±0.04	7.53±3.54	0.13	9.08±0.01	0.38	0.07±0.01	16.96±7.46	0.14
5		4.93	5.13	1.42	2.71	14.37±0.02	0.57	0.11±0.03	6.70±3.07	0.08	8.77±0.02	0.34	0.06±0.02	0.86±0.35	0.11
6		4.88	10.06	1.42	2.49	12.38±0.01	0.51	0.10±0.03	7.46±3.14	0.13	7.01±0.01	0.23	0.09±0.04	0.82±0.44	0.10
7	Pb <sup>2+</sup> -Zn <sup>2+</sup>	5.26	2.91	1.42	2.69	13.01±0.01	0.55	0.12±0.01	6.03±0.17	0.12	6.33±0.02	0.35	0.03±0.01	5.77±1.83	0.08
8		5.22	5.36	1.42	2.71	12.51±0.01	0.45	0.10±0.02	9.56±2.44	0.08	4.25±0.02	0.27	0.07±0.01	5.05±1.14	0.05
9		5.41	9.67	1.42	2.49	9.01±0.02	0.40	0.09±0.04	4.12±2.25	0.13	4.64±0.02	0.14	0.08±0.02	0.45±0.18	0.09
10		4.33 <sup>†</sup>	9.48	1.42	2.35	7.46±0.03	0.67	0.08±0.03	5.80±2.73	0.18	2.61±0.05	0.25	0.08±0.03	1.32±0.53	0.07
11	Pb <sup>2+</sup> -Mn <sup>2+</sup>	5.31	2.73	1.42	2.84	13.19±0.01	0.46	0.12±0.02	8.13±2.63	0.11	6.33±0.04	0.28	0.03±0.01	6.50±2.51	0.08
12		5.14	4.47	1.42	2.46	10.68±0.01	0.34	0.08±0.01	1.86±0.13	0.12	5.40±0.01	0.19	0.05±0.01	4.00±1.16	0.07
13		4.85	8.66	1.42	2.70	10.33±0.01	0.48	0.08±0.02	6.61±2.37	0.10	3.77±0.20	0.30	0.05±0.03	1.60±1.08	0.10
14	Pb <sup>2+</sup> -Zn <sup>2+</sup> - Ni <sup>2+</sup> -Mn <sup>2+</sup>	4.56	Zn <sup>2+</sup> =4.73 Ni <sup>2+</sup> =5.19 Mn <sup>2+</sup> =4.38	1.42	2.60	8.38±0.93	0.25	5.16±0.01	3.61±1.45	0.09	5.16±0.01	0.13	0.04±0.01	0.56±0.20	0.07
											5.49±0.01	0.19	0.04±0.02	1.87±0.88	0.06
											5.05±0.01	0.16	0.03±0.01	1.39±0.56	0.07

<sup>†</sup>dispersivity derived from tracer test ; \* average dispersivity derived from average of dispersivity values of 3 tracer columns <sup>†</sup>Pb's column derived from chapter 4; <sup>##</sup>Duplicated column

**Table 5.4** Estimated transport parameters for heavy metal breakthrough curves using linear and Langmuir isotherm from nonequilibrium convection-dispersion approaches (two-site model, TSM) generated by HYDRUS-1D

No	System	$C_0$ (mM)		$\lambda^{\pm}$ (cm)	Measured $\nu$ (cm hr <sup>-1</sup> )	Nonequilibrium model fit (TSM)									
		1 <sup>st</sup> metal (Pb <sup>2+</sup> )	2 <sup>nd</sup> metal			1 <sup>st</sup> metal					2 <sup>nd</sup> metal				
						$Q_{max\pm 95\%CI}$ (mM g <sup>-1</sup> )	$b\pm 95\%CI$ (L mM <sup>-1</sup> )	$f$ $\pm 95\%CI$	$\alpha\pm 95\%CI$ (hr <sup>-1</sup> )	SSE	$Q_{max\pm 95\%CI}$ (mM g <sup>-1</sup> )	$b\pm 95\%CI$ (L mM <sup>-1</sup> )	$f$ $\pm 95\%CI$	$\alpha\pm 95\%CI$ (hr <sup>-1</sup> )	SSE
1															
2		5.05*	0	1.42	2.55	0.20±0.04	3.34±0.78	0.31±0.05	0.011±0.001	0.020	-	-	-	-	-
3		5.01*	0	0.97	2.55	0.20±0.04	2.39±0.54	0.42±0.12	0.012±0.005	0.044	-	-	-	-	-
4	Pb <sup>2+</sup> -	4.86	3.01	1.42	2.72	0.13±0.03	3.29±0.86	0.39±0.10	0.017±0.006	0.029	0.06±0.02	3.36±1.21	0.31±0.11	0.029±0.010	0.03
5	Ni <sup>2+</sup>	4.85 <sup>z</sup>	3.17	1.57	2.82	0.14±0.01	3.91±0.32	0.34±0.07	0.014±0.004	0.027	0.06±0.02	6.11±1.77	0.41±0.10	0.025±0.011	0.03
		4.93	5.13	1.42	2.71	0.12±0.04	4.65±1.42	0.40±0.10	0.020±0.006	0.021	0.08±0.02	2.33±0.67	0.43±0.18	0.075±0.028	0.03
		4.88	10.06	1.42	2.49	0.11±0.06	3.47±1.79	0.42±0.13	0.017±0.009	0.046	0.11±0.01	0.64±0.08	0.49±0.20	0.054±0.001	0.05
6		5.26	2.91	1.42	2.69	0.12±0.02	2.97±1.08	0.34±0.11	0.021±0.007	0.038	0.04±0.02	3.28±1.32	0.37±0.11	0.030±0.014	0.04
7	Pb <sup>2+</sup> -	5.22	5.36	1.42	2.71	0.11±0.02	3.43±0.77	0.38±0.11	0.024±0.009	0.031	0.06±0.02	2.27±0.85	0.45±0.17	0.040±0.027	0.03
8	Zn <sup>2+</sup>	5.41	9.67	1.42	2.49	0.09±0.03	2.22±0.91	0.52±0.14	0.027±0.018	0.046	0.10±0.06	0.37±0.22	0.58±0.19	0.047±0.039	0.05
9		4.33 <sup>z</sup>	9.48	1.42	2.35	0.09±0.03	2.71±0.73	0.35±0.14	0.021±0.012	0.069	0.10±0.03	0.72±0.15	0.38±0.14	0.038±0.025	0.04
10	Pb <sup>2+</sup> -	5.31	2.73	1.42	2.84	0.12±0.05	3.21±1.24	0.35±0.12	0.022±0.010	0.042	0.04±0.01	3.55±0.08	0.38±0.07	0.023±0.008	0.03
11	Mn <sup>2+</sup>	5.14	4.47	1.42	2.46	0.09±0.04	3.03±1.26	0.48±0.02	0.030±0.014	0.039	0.05±0.03	1.61±0.98	0.47±0.14	0.040±0.002	0.04
12		4.85	8.66	1.42	2.70	0.10±0.05	3.24±1.53	0.31±0.12	0.022±0.008	0.037	0.10±0.05	1.42±0.61	0.31±0.09	0.029±0.012	0.03
	Pb <sup>2+</sup> -														
	Zn <sup>2+</sup> -	4.56	Zn <sup>2+</sup> =4.73	1.42	2.60	0.08±0.02	1.83±0.42	0.48±0.07	0.028±0.019	0.051	0.04±0.01	0.60±0.26	0.55±0.21	0.062±0.064	0.04
13	Ni <sup>2+</sup> -		Ni <sup>2+</sup> =5.19								0.05±0.01	1.08±0.30	0.46±0.10	0.048±0.028	0.03
	Mn <sup>2+</sup>		Mn <sup>2+</sup> =4.38								0.04±0.01	0.88±0.28	0.48±0.12	0.051±0.037	0.04

<sup>†</sup>dispersivity derived from tracer test; <sup>\*</sup> average dispersivity derived from average of dispersivity values of 3 tracer columns <sup>\*</sup>Pb's column derived from chapter 4; <sup>z</sup>Duplicated column



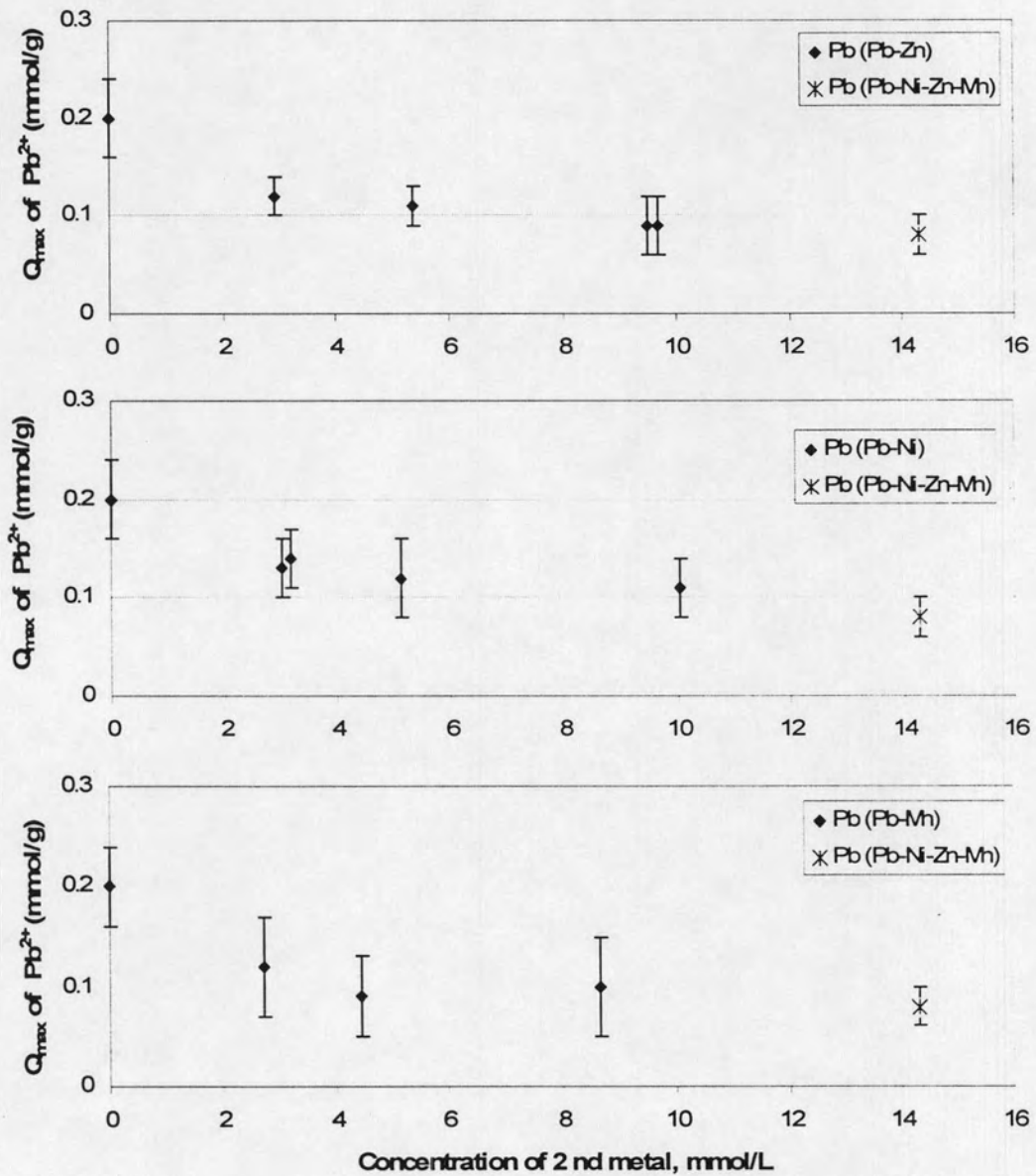


Figure 5.16 Maximum sorption capacity,  $Q_{max}$ , of  $Pb^{2+}$  with increasing initial concentration of 2<sup>nd</sup> metal in binary and multiple metal systems

## 5.4 Conclusion

Based on the breakthrough times of  $Pb^{2+}$  in single metal system,  $Pb^{2+}$  was found to be retained in lateritic soil more than the other metals ( $Zn^{2+}$ ,  $Ni^{2+}$ , and  $Mn^{2+}$ ), resulting in retardation factors and averaged maximum sorption capacity that are higher than the other tested metals for single, binary and multi-metal systems. However, due to the presence of other metals ( $Zn^{2+}$ ,  $Ni^{2+}$ , and  $Mn^{2+}$ ) in the binary and multi-metal system, competition for available sorption sites resulted in decreasing maximum sorption capacity of individual metals for both binary and multi-metal system.

Use of local equilibrium convection-dispersion model with linear and Langmuir isotherm did not describe the rising and declining limbs of metal concentration in binary and multi-metal systems. The more complex model, two-site model (TSM) described the rising limb and initial declining limb well but could not explain the extended tailing phenomenon. This might be due to the rate of sorption/desorption from the sorption sites which may not be described by a first-order rate constant or there may be more one type of sorption/desorption kinetics that needs to be considered in addition to the instantaneous sorption sites. The curve-fitted results of the TSM chemical nonequilibrium two-site model for individual metals in binary and multi-metal systems were found to be statistically different from the results of the equilibrium convection-dispersion model indicating that the TSM presented a better agreement with the experimental results (statistically significantly,  $P < 0.05$ ). These results reinforce the necessity of using transport models and proper parameters to predict heavy metal transport more accurately in field condition and more efficiently in selecting the appropriate strategies in remediation/monitoring the heavy metal contaminated site.